**EPJ manuscript No.**
(will be inserted by the editor)

# Dependence of the triple-alpha process on the fundamental constants of nature

Evgeny Epelbaum[1], Hermann Krebs[1], Timo A. Lähde[2], Dean Lee[3], and Ulf-G. Meißner[2,4,5]

[1] Institut für Theoretische Physik II, Ruhr-Universität Bochum, D-44870 Bochum, Germany
[2] Institut für Kernphysik, Institute for Advanced Simulation, Jülich Center for Hadron Physics, Forschungszentrum Jülich, D-52425 Jülich, Germany
[3] Department of Physics, North Carolina State University, Raleigh, NC 27695, USA
[4] JARA – High Performance Computing, Forschungszentrum Jülich, D-52425 Jülich, Germany
[5] Helmholtz-Institut für Strahlen- und Kernphysik and Bethe Center for Theoretical Physics, Universität Bonn, D-53115 Bonn, Germany

Received: date / Revised version: date

**Abstract.** We present an *ab initio* calculation of the quark mass dependence of the ground state energies of $^4$He, $^8$Be and $^{12}$C, and of the energy of the Hoyle state in $^{12}$C. These investigations are performed within the framework of lattice chiral Effective Field Theory. We address the sensitivity of the production rate of carbon and oxygen in red giant stars to the fundamental constants of nature by considering the impact of variations in the light quark masses and the electromagnetic fine-structure constant on the reaction rate of the triple-alpha process. As carbon and oxygen are essential to life as we know it, we also discuss the implications of our findings for an anthropic view of the Universe. We find strong evidence that the physics of the triple-alpha process is driven by alpha clustering, and that shifts in the fundamental parameters at the $\simeq 2-3\%$ level are unlikely to be detrimental to the development of life. Tolerance against much larger changes cannot be ruled out at present, given the relatively limited knowledge of the quark mass dependence of the two-nucleon $S$–wave scattering parameters. Lattice QCD is expected to provide refined estimates of the scattering parameters in the future.

**PACS.** 21.10.Dr – 21.30.-x – 21.45.-v – 21.60.De – 26.20.Fj

arXiv:1303.4856v2 [nucl-th] 2 Sep 2013

## 1 Introduction

The "Hoyle state" is an excited state of $^{12}$C with quantum numbers $J^p = 0^+$ just above the $^8$Be–$\alpha$ threshold. The existence of such a state was predicted by Hoyle in order to explain the observed abundance of $^{12}$C, which is produced during helium burning in red giant stars via the so-called triple-alpha process. In this two-step process, two $^4$He nuclei first combine to form the unstable, but relatively long-lived (under the conditions prevalent in the cores of red giant stars) $^8$Be nucleus. This resonance must then combine with a third alpha particle in order to generate carbon.

However, the fact that this process cannot by itself explain the observed abundance of $^{12}$C in the Universe motivated Hoyle in 1954 to propose the existence of an excited $0^+$ state of $^{12}$C, just above the $^8$Be–$\alpha$ threshold. Such a resonant enhancement could then provide a sufficiently high rate of production of $^{12}$C to account for the observed abundance [1]. Soon afterwards, the predicted state was detected at Caltech [2,3], and the modern value for its energy is $\varepsilon = 379.47(18)$ keV relative to the $3\alpha$ threshold, while the total and radiative widths are $\Gamma_{\rm tot} = 8.3(1.0)$ eV and $\Gamma_\gamma = 3.7(5)$ meV.

While the Hoyle state dramatically increases the reaction rate of the triple-alpha process, the resulting enhancement is also extremely sensitive to the exact value of $\varepsilon$, which is therefore the principal control parameter of this reaction. As the Hoyle state is crucial to the formation of elements essential to life as we know it, this state has been nicknamed the "level of life" [4] Thus, the Hoyle state is often viewed as a prime manifestation of the anthropic principle, which states that the observable values of the fundamental physical and cosmological parameters are restricted by the requirement that life can form to determine them, and that the Universe be old enough for that to occur [6,7]. See, however, Ref. [5] for a thorough historical discussion of the Hoyle state in view of the anthropic principle. We remark that in the context of cosmology and string theory, the anthropic principle and its consequences have had a significant influence (see *e.g.* Refs. [8,9]).

The impact of changes in the energy of the Hoyle state on the synthesis of $^{12}$C and $^{16}$O in red giant stars has been investigated in several numerical studies that make

use of highly sophisticated stellar evolution models. Livio *et al.* [10] modified the value of $\varepsilon$ by hand and studied the triple-alpha process in the core and shell helium burning up to the asymptotic giant branch stage in the stellar evolution. These calculations have been refined by Oberhummer *et al.*, who concluded that the production of either $^{12}$C or $^{16}$O becomes strongly suppressed for changes larger than $\delta(\varepsilon) \simeq \pm 100$ keV in the position of the Hoyle state [11]. In essence, if $\varepsilon$ is lowered too much, the triple-alpha process ignites at a significantly lower stellar core temperature, and hence not much energy is available for the process $^{12}\mathrm{C} + {}^4\mathrm{He} \to {}^{16}\mathrm{O} + \gamma$. Conversely, if $\varepsilon$ is raised too much, the triple-alpha process ignites at a much higher core temperature, and hence most of the $^{12}$C formed is immediately converted into $^{16}$O and $^{20}$Ne already before the conclusion of core He burning. However, since a $\simeq 100$ keV change in $\varepsilon$ could still be tolerated, which is a 25% modification, the degree of fine-tuning was revealed to not be as severe as was first believed [14].

In addition to these *ad hoc* changes in $\varepsilon$, a more microscopic calculation was performed by Oberhummer *et al.* [12,13] in terms of a nuclear cluster model based on a simple nucleon-nucleon (NN) interaction with inclusion of electromagnetic (EM) effects. This NN interaction was formulated in terms of one strength parameter adjusted to give a fair description of $\alpha$–$\alpha$ scattering and the spectrum of $^{12}$C. By modifying this coupling strength and the EM fine structure constant $\alpha_{\rm em}$, the effect on the stellar production of $^{12}$C and $^{16}$O was analyzed. Within such a model, an adequate amount of $^{12}$C and $^{16}$O was produced within a relatively narrow window of $\simeq 0.5\%$ around the observed strong force and of $\simeq 4\%$ around the observed strength of the EM interaction. For larger changes, the stellar production of carbon and/or oxygen was found to be reduced by several orders of magnitude.

However, the translation of the findings of Ref. [13] into anthropic constraints on fundamental parameters remains problematic, as the employed model of the strong force is not readily connected to the fundamental theory of the strong interactions, Quantum Chromodynamics (QCD) and its fundamental parameters, the light quark masses. In this study, we address this question by means of an *ab initio* calculation of the sensitivity of $\varepsilon$ to changes in the light quark masses and the EM fine structure constant $\alpha_{\rm em}$. For this purpose, we carry out large-scale numerical lattice calculations for the energies and energy differences relevant to the triple-alpha process within the framework of chiral Effective Field Theory (EFT). The discretized (lattice) version of chiral EFT was formulated in Ref. [15] (see Ref. [16] for a recent review). We have successfully applied this novel approach to the spectra and properties of light nuclei [17,18,19,20], to dilute neutron matter [21], and to the structure of the Hoyle state [22]. A brief summary of the results reported here has appeared in Ref. [23].

This paper is organized as follows: In Section 2, we briefly describe the theoretical framework of the present calculation. The quark mass dependence of the nuclear force is described in Section 3 within the framework of chiral EFT, in combination with lattice QCD calculations. The analysis of the NN system is carried out in Section 4, while Section 5 deals with the Auxiliary Field Quantum Monte Carlo (AFQMC) calculation of the energies of the $^4$He, $^8$Be and $^{12}$C ground states as well as the Hoyle state, including the energy differences relevant for the triple-alpha process. Section 6 provides an estimation of the neglected higher-order effects, while the observed correlations between the relevant energies and energy differences are described in Section 7. Finally, in Section 8 the implications of our findings for the reaction rate of the triple-alpha process are discussed, and Section 9 contains a concluding summary.

## 2 Theoretical framework

As discussed above, the triple-alpha reaction proceeds in two steps. The reaction rate of the first step $^4$He + $^4$He $\to$ $^8$Be, where the unstable $^8$Be resonance is formed, is controlled by the energy difference $\Delta E_b$,

$$\Delta E_b \equiv E_8 - 2E_4, \tag{1}$$

where we have introduced the notations $E_4$ and $E_8$ for the energies of the ground states of $^4$He and $^8$Be, respectively. Also, we shall denote the ground state energy of $^{12}$C by $E_{12}$, and the energy of the Hoyle state by $E_{12}^\star$. The second step in the triple-alpha process, $^8\mathrm{Be} + {}^4\mathrm{He} \to {}^{12}\mathrm{C} + \gamma$, depends crucially on the energy difference $\Delta E_h$,

$$\Delta E_h \equiv E_{12}^\star - E_8 - E_4, \tag{2}$$

such that the reaction rate for fusion of three $\alpha$ particles to $^{12}$C via the ground state of $^8$Be and the Hoyle state is given by [13]

$$r_{3\alpha} = 3^{\frac{3}{2}} N_\alpha^3 \left(\frac{2\pi\hbar^2}{|E_4| k_{\rm B} T}\right)^3 \frac{\Gamma_\gamma}{\hbar} \exp\left(-\frac{\varepsilon}{k_{\rm B} T}\right), \tag{3}$$

where $N_\alpha$ is the number density of $\alpha$ particles in a stellar plasma at temperature $T$. The energy difference $\varepsilon$ is given by

$$\varepsilon \equiv \Delta E_b + \Delta E_h = E_{12}^\star - 3E_4, \tag{4}$$

which clearly is the dominant control parameter of Eq. (3) in comparison with the linear dependence on the radiative width $\Gamma_\gamma$ of the Hoyle state. The latter can therefore be neglected when the impact of small changes in $\varepsilon$ on $r_{3\alpha}$ are considered.

The main question we shall address here is the sensitivity of $\varepsilon$ to variations in the light quark masses and the EM fine structure constant, with the objective of translating the bounds on $\varepsilon$ found in the stellar model calculations of Ref. [13,24] to constraints on these fundamental parameters. For this purpose, we shall only consider the average light quark mass $m_q \equiv (m_u + m_d)/2$, as the effects of strong isospin violation due to $m_u \neq m_d$ are greatly suppressed for the processes of relevance to the present work. To this end, we shall calculate how $E_4$, $E_8$, $E_{12}$ and $E_{12}^\star$ depend on $m_q$ and $\alpha_{\rm em}$, after which we may use this information to determine the corresponding dependences of $\Delta E_b$, $\Delta E_h$ and $\varepsilon$.

Our analysis is carried out within the framework of chiral nuclear EFT, introduced by Weinberg [25] as a systematic tool to explore the consequences of spontaneous and explicit chiral symmetry breaking of QCD in a rigorous manner. This approach relies on the most general effective Lagrangian for pions and nucleons constructed in harmony with the symmetries of QCD. The pions are identified with the pseudo-Goldstone bosons of the spontaneously broken chiral symmetry of QCD, which strongly constrains their interactions. The small (but non-vanishing) pion mass is a result of the explicit breaking of chiral symmetry in QCD by the quark masses. In particular, one finds $M_\pi^2 \sim (m_u + m_d)$, so that any dependence on the average light quark mass $m_q$ can be translated into a corresponding dependence on the pion mass $M_\pi$.

Chiral nuclear EFT is based on an order-by-order expansion of the nuclear potential. In this scheme, two-, three- and four-nucleon forces arise naturally, and their observed hierarchy of importance is also explained. The nuclear forces have been worked out to high precision and applied successfully in few-nucleon systems to the binding energies, structure, and reactions (see Refs. [26,27] for recent reviews). We have recently developed a discretized version of chiral EFT which allows one to compute the correlation function

$$Z_A(t) = \langle \Psi_A | \exp(-tH) | \Psi_A \rangle, \tag{5}$$

for $A$ nucleons in Euclidean space-time using Monte Carlo sampling. Here, $\Psi_A$ denotes the Slater determinant for $A$ non-interacting nucleons, and $H$ is the nuclear Hamiltonian calculated in chiral EFT and expressed in terms of the lattice (discretized) variables. The correlation function $Z_A(t)$ can be efficiently calculated within the AFQMC framework, where terms in the lattice action quartic in the nucleon fields are re-expressed as interactions of a single nucleon with auxiliary fields by means of a Hubbard-Stratonovich transformation. Once $Z_A(t)$ has been calculated, the ground-state energy $E_A$ is obtained from the large-$t$ limit of $Z_A$,

$$E_A = -\lim_{t\to\infty} \frac{d(\ln Z_A)}{dt}, \tag{6}$$

with $t$ the Euclidean time. We have also developed a multi-channel projection Monte Carlo method, which allows us to study excited states by computing the correlation matrix for a set of $A$–nucleon states $\Psi_A^i$ with appropriately chosen quantum numbers,

$$Z_A^{ij}(t) = \langle \Psi_A^i | \exp(-tH) | \Psi_A^j \rangle. \tag{7}$$

The AFQMC results reported here correspond to an improved leading-order (LO) action, based on the NN amplitude

$$\begin{aligned}\mathcal{A}_{\rm LO} = {} & C_{S=0,I=1}\, f(\boldsymbol{q}) \left(\frac{1}{4} - \frac{1}{4}\,\boldsymbol{\sigma}_i\cdot\boldsymbol{\sigma}_j\right)\left(\frac{3}{4} + \frac{1}{4}\,\boldsymbol{\tau}_i\cdot\boldsymbol{\tau}_j\right) \\ & + C_{S=1,I=0}\, f(\boldsymbol{q}) \left(\frac{3}{4} + \frac{1}{4}\,\boldsymbol{\sigma}_i\cdot\boldsymbol{\sigma}_j\right)\left(\frac{1}{4} - \frac{1}{4}\,\boldsymbol{\tau}_i\cdot\boldsymbol{\tau}_j\right) \\ & - \tilde{g}_{\pi N}^2\, \boldsymbol{\tau}_i\cdot\boldsymbol{\tau}_j\, \frac{\boldsymbol{\sigma}_i\cdot\boldsymbol{q}\,\boldsymbol{\sigma}_j\cdot\boldsymbol{q}}{\boldsymbol{q}^2 + M_\pi^2},\end{aligned} \tag{8}$$

where $\boldsymbol{\sigma}_i$ and $\boldsymbol{\tau}_i$ refer to the Pauli spin and isospin matrices of nucleon $i$, respectively. The strength $\tilde{g}_{\pi N}$ of the one-pion exchange potential is defined in terms of the nucleon axial-vector coupling $g_A$ and the pion decay constant $F_\pi$ as

$$\tilde{g}_{\pi N} \equiv \frac{g_A}{2F_\pi}, \tag{9}$$

while $C_{S=0,I=1}$ and $C_{S=1,I=0}$ are low-energy constants (LECs), adjusted to reproduce the NN phase shifts in the ${}^1S_0$ and ${}^3S_1$ partial waves respectively. The smearing function $f(\boldsymbol{q})$ is chosen to give the (approximately) correct effective ranges for the two $S$–wave NN channels (see Ref. [19] and references therein for more details, along with a description of the discretized form of the improved LO action). Corrections of higher order are taken into account in perturbation theory. In this analysis, we only consider small momentum-independent changes to the short-range interactions. These correspond to pointlike contact operators, and it is convenient to express the LECs in terms of the linear combinations $C_0$ and $C_I$,

$$C_0 = \frac{3}{4}\, C_{S=0,I=1} + \frac{1}{4}\, C_{S=1,I=0}, \tag{10}$$

$$C_I = \frac{1}{4}\, C_{S=0,I=1} - \frac{1}{4}\, C_{S=1,I=0}, \tag{11}$$

which couple to the total nucleon density and the isospin density $\boldsymbol{\tau}_i\cdot\boldsymbol{\tau}_j$, respectively.

The expectation value of a given operator $\mathcal{O}$ is obtained as

$$Z_A^{\mathcal{O}}(t) = \langle \Psi_A | \exp(-tH/2)\, \mathcal{O}\, \exp(-tH/2) | \Psi_A \rangle, \tag{12}$$

which accounts for all contributions to the nuclear Hamiltonian up to next-to-next-to-leading order ($\mathrm{N^2LO}$) in the chiral expansion, including the Coulomb interaction and the three-nucleon forces. Our recent AFQMC calculations using this framework are reported in Refs. [17,18,19,20,22]. In particular, results at $\mathrm{N^2LO}$ for nuclei with $A = 3, 4, 6$ and 12 can be found in Ref. [19]. These calculations employ a periodic cubic lattice with a lattice spacing of $a = 1.97$ fm and a length of $L = 11.82$ fm. In the (discretized) Euclidean time direction, we use a step size of $a_t = 1.32$ fm, and perform calculations for propagation times, *i.e.* the extent of the time direction, $L_t \equiv N_t a_t = 4 \ldots 20$ fm, such that the limit $L_t \to \infty$ is taken by extrapolation. Given the relatively coarse lattice spacing employed in our calculations, the two-pion exchange NN potential that starts contributing at next-to-leading order (NLO) can be well represented by contact interactions [19].

We now turn to the $m_q$-dependence or, equivalently, the $M_\pi$-dependence of the energies $E_i$. We use the notation $E_i$ when referring to either the energies $E_4$, $E_8$, $E_{12}$ and $E_{12}^\star$, or to the energy differences $\Delta E_b$, $\Delta E_h$ and $\varepsilon$. In this work, we shall restrict the values of $M_\pi$ to the vicinity of the physical pion mass, roughly speaking to $|\delta M_\pi / M_\pi| \le 10\%$. It is then sufficient to consider the linear variation of $E_i$, giving

$$\delta E_i \simeq \left.\frac{\partial E_i}{\partial M_\pi}\right|_{M_\pi^{\rm ph}} \delta M_\pi + \left.\frac{\partial E_i}{\partial \alpha_{\rm em}}\right|_{\alpha_{\rm em}^{\rm ph}} \delta\alpha_{\rm em}, \tag{13}$$

where we have allowed for independent variations of $M_\pi$ and $\alpha_{\rm em}$. Our objective is then to compute the partial derivatives in Eq. (13) using AFQMC. Clearly, such a calculation relies on knowledge of the $M_\pi$-dependence of the nuclear Hamiltonian, which is discussed in Section 3. We also note that a useful way to express the sensitivity of a given observable $X$ to a parameter $y$ is given by the dimensionless "$K$-factors"

$$K_X^i \equiv \frac{y}{X}\,\frac{\partial X}{\partial y}\bigg|_{y^{\rm ph}}\,, \tag{14}$$

where we use the superscript $i = \{q,\, \pi,\, \alpha\}$ for the set of observables $y = \{m_q,\, M_\pi,\, \alpha_{\rm em}\}$. As an example, we can obtain $K_X^q$ (*i.e.* the sensitivity of $X$ to changes in $m_q$) in terms of $K_X^\pi$ by means of the relation

$$K_X^q = K_X^\pi K_{M_\pi}^q\,, \tag{15}$$

where we shall adopt the value $K_{M_\pi}^q = 0.494^{+0.009}_{-0.013}$ from Ref. [28].

In addition to shifts in $m_q$, we shall also consider the effects of shifts in $\alpha_{\rm em}$. The treatment of the Coulomb interaction in our AFQMC framework is described in detail in Ref. [19]. The main difference between the continuum and lattice formulations is that the discretized form of the long-range Coulomb force between two protons becomes singular if the protons occupy the same lattice site. We therefore employ a regularized version of the discretized Coulomb interaction, where the potential energy of two protons on the same lattice site is set to the continuum value corresponding to a separation of half a lattice spacing. The effects of this regularization are compensated for by a derivative-less proton-proton contact operator, which also receives contributions from the strong and short-range EM isospin-breaking effects. The associated coefficient $c_{pp}$ is determined from the proton-proton phase shifts.

The sensitivity of the energies $E_i$ to variations in $\alpha_{\rm em}$ can be obtained by computing the shifts $\Delta E_i(\alpha_{\rm em})$ and $\Delta E_i(c_{pp})$. The former is due to the long-range Coulomb interaction on the lattice, and the latter arises from the part of the proton-proton contact operator $\propto c_{pp}$. Specifically, we define

$$Q_{\rm em}(E_i) \equiv \Delta E_i(c_{pp})\, x_{pp} + \Delta E_i(\alpha_{\rm em}), \tag{16}$$

where the coefficient $x_{pp}$ denotes the relative strength of the $pp$ contact interaction caused by the regularization of the Coulomb force. The determination of $x_{pp}$ will be described in Section 5. Given that the energy shifts $\Delta E_i(\alpha_{\rm em})$ and $\Delta E_i(c_{pp})$ are relatively small, we may approximate

$$\frac{\partial E_i}{\partial \alpha_{\rm em}}\bigg|_{\alpha_{\rm em}^{\rm ph}} \simeq \frac{Q_{\rm em}(E_i)}{\alpha_{\rm em}^{\rm ph}}, \tag{17}$$

with $\alpha_{\rm em}^{\rm ph} \simeq 1/137$. While we shall mainly study the explicit dependence on $\alpha_{\rm em}$ induced by the Coulomb interaction, it is worth noting that $K_X^\alpha$ may receive additional contributions from the corresponding shifts in the effective hadronic Lagrangian, for example from the EM shift of $M_\pi$. Schematically, this may be expressed as

$$K_X^\alpha = \frac{Q_{\rm em}(X)}{X} + \frac{\Delta M_\pi^{\rm em}}{X}\,\frac{\partial X}{\partial M_\pi}\bigg|_{M_\pi^{\rm ph}} + \ldots, \tag{18}$$

where the sizes of such additional contributions to the EM $K$-factors are $\Delta M_\pi^{\rm em}/M_\pi \simeq 4\%$ compared to the dominant strong contributions, and are thus not considered in the present analysis.

## 3 Pion mass dependence of the nuclear Hamiltonian

The $M_\pi$-dependence of the energies $E_i$ is generated by the $M_\pi$-dependence of the nucleon mass $m_N$ in the kinetic energy term in the nuclear Hamiltonian, as well as by the $M_\pi$-dependence of the nuclear potentials. In the present analysis, we will not take into account the sources of $M_\pi$-dependence generated by contributions beyond $\mathcal{A}_{\rm LO}$ in Eq. (8). Instead, we shall estimate the neglected higher-order contributions to the energy shifts in Section 6. On the other hand, in order to obtain the most accurate description possible of the $M_\pi$-dependence of $\mathcal{A}_{\rm LO}$ and to ensure model independence, we shall go beyond the strict chiral expansion of the terms entering Eq. (8), and make use of the available lattice QCD data whenever possible.

For the $M_\pi$-dependence of the nucleon mass, we define the quantity

$$x_1 \equiv \frac{\partial m_N}{\partial M_\pi}\bigg|_{M_\pi^{\rm ph}}\,, \tag{19}$$

which has been analyzed extensively in the literature by combining Chiral Perturbation Theory (ChPT) with lattice QCD data, see *e.g.* Ref. [29,30]. At $\mathcal{O}(p^2)$ in ChPT, $m_N(M_\pi)$ is given by

$$m_N = m_0 - 4c_1 M_\pi^2 + \mathcal{O}(p^3), \tag{20}$$

where $m_0$ denotes the value of $m_N$ in the chiral limit. The value $x_1 \simeq 0.57$ was obtained in Ref. [28], which corresponds to the $\mathcal{O}(p^3)$ heavy-baryon (HB) ChPT result with $c_1 = -0.81$ GeV$^{-1}$. Alternatively, one may determine $x_1$ from the pion-nucleon sigma term $\sigma_{\pi N} \equiv M_\pi^2\, \partial m_N/\partial M_\pi^2$ by means of the Feynman-Hellmann theorem. From the results of Ref. [50], one finds

$$\sigma_{\pi N} = 44.9^{+1.8}_{-5.4}\ {\rm MeV} \quad \to \quad x_1 = 0.66^{+0.02}_{-0.08}, \tag{21}$$

while those of Ref. [51] yield

$$\sigma_{\pi N} = 59 \pm 7\ {\rm MeV} \quad \to \quad x_1 = 0.87 \pm 0.10, \tag{22}$$

and we also note that $x_1 \simeq 0.73$ has been obtained by Procura *et al.* from fits of a modified $\mathcal{O}(p^4)$ ChPT formula to lattice QCD data [29]. In our analysis, we adopt the conservative estimate

$$x_1 = 0.57 \ldots 0.97, \tag{23}$$

based on the variation in the results quoted above.

We now turn to the $M_\pi$-dependence of the nuclear force. The most obvious source of $M_\pi$-dependence is the static pion propagator in Eq. (8). In addition to this explicit dependence on $M_\pi$, we also take into account the implicit $M_\pi$-dependence of the coupling constant $\tilde{g}_{\pi N}$ of the one-pion exchange (OPE) potential by defining

$$x_2 \equiv \left.\frac{\partial \tilde{g}_{\pi N}}{\partial M_\pi}\right|_{M_\pi^{\rm ph}} = \frac{1}{2F_\pi}\left.\frac{\partial g_A}{\partial M_\pi}\right|_{M_\pi^{\rm ph}} - \frac{g_A}{2F_\pi^2}\left.\frac{\partial F_\pi}{\partial M_\pi}\right|_{M_\pi^{\rm ph}}, \tag{24}$$

where both contributions to $x_2$ have been studied extensively by means of ChPT and lattice QCD (see Refs. [28, 30,31] and references therein). As for $m_N$ in Eq. (20), we obtain

$$F_\pi = F\left(1 + \frac{M_\pi^2}{16\pi^2 F^2}\bar{l}_4 + \mathcal{O}(M_\pi^4)\right), \tag{25}$$

where we use $\bar{l}_4 \simeq 4.3$ from Ref. [32], which is consistent with modern lattice determinations, see e.g. Ref. [33], $\bar{l}_4 = 4.67(3)(10)$, and $F \simeq 86.2$ MeV is the value of $F_\pi$ in the chiral limit. As an alternative to the sub-leading order ChPT result, one may use the determination of $K^q_{F_\pi}$ reported in Ref. [28], $K^q_{F_\pi} = 0.048 \pm 0.012$, which is based on a combined analysis in ChPT and lattice QCD. This gives

$$\left.\frac{\partial F_\pi}{\partial M_\pi}\right|_{M_\pi^{\rm ph}} = \frac{F_\pi}{M_\pi}\frac{K^q_{F_\pi}}{K^q_{M_\pi}} \simeq 0.066, \tag{26}$$

using the central value $K^q_{M_\pi} = 0.494$, as discussed in Section 2.

While the chiral expansion of $F_\pi$ shows good convergence, the equivalent expression for $g_A$ is known to converge much slower. In particular, the $\mathcal{O}(p^3)$ HB ChPT result for $g_A$ shows a very strong $M_\pi$-dependence near the physical point (see Refs. [28,34] and references therein). On the other hand, lattice QCD calculations indicate that $g_A$ as a function of $M_\pi$ is remarkably flat. In principle, such flat behavior can be accommodated at the two-loop level in ChPT [28]. By assuming that $g_A$ is constant in the vicinity of the physical point, the value $x_2 \simeq -0.049$ in lattice units (l.u.) is obtained from Eq. (24). This should be compared with the central value reported in Ref. [28], $x_2 = -0.024$ l.u., which is obtained from the incomplete $\mathcal{O}(p^4)$ HB result for $g_A$, constrained by the available lattice QCD result at $M_\pi \simeq 350$ MeV. The relatively large uncertainty in the chiral extrapolation of $g_A$ has a significant impact on the allowed values of $x_2$. The largest source of uncertainty in Ref. [28] is the poorly known low-energy constant $\bar{d}_{16}$. The present empirical constraints from the reaction $\pi N \to \pi\pi N$ yield a relatively large range of $\bar{d}_{16} = -0.91 \ldots -2.61$ GeV$^{-2}$, which in turn gives

$$x_2 = -0.056 \ldots 0.008 \text{ l.u.}, \tag{27}$$

for the range of uncertainty in $x_2$, which we shall adopt in the present analysis.

The short-range part of the nuclear force also depends on $M_\pi$. This dependence is more difficult to control within chiral EFT, see Ref. [28] for an extended discussion. Since we aim at a model-independent determination of the $M_\pi$-dependence of the nuclear energies $E_i$, we refrain from a chiral expansion of the short-range part of the nuclear force. Rather, we shall *parameterize* the $M_\pi$-dependence of the LO contact interactions, *i.e.* of the coefficients $C_0$ and $C_I$ in Eq. (8). This can be performed in terms of the slope of the inverse NN $S$–wave scattering lengths $a_s^{-1}$ and $a_t^{-1}$,

$$\bar{A}_s \equiv \left.\frac{\partial a_s^{-1}}{\partial M_\pi}\right|_{M_\pi^{\rm ph}}, \quad \bar{A}_t \equiv \left.\frac{\partial a_t^{-1}}{\partial M_\pi}\right|_{M_\pi^{\rm ph}}, \tag{28}$$

where we have introduced the subscripts $s$ and $t$ for the spin–0 ($^1S_0$) and spin–1 ($^3S_1$) NN partial waves. For the purpose of our analysis, $\bar{A}_s$ and $\bar{A}_t$ are regarded as input parameters, and we shall express all our results in terms of these. We shall return to the determination of $\bar{A}_s$ and $\bar{A}_t$ in Section 8.

Given the sources of $M_\pi$-dependence discussed so far, we may express the dependence of the energies $E_i$ on $M_\pi$ as

$$E_i = E_i(\tilde{M}_\pi, m_N(M_\pi), \tilde{g}_{\pi N}(M_\pi), C_0(M_\pi), C_I(M_\pi)), \tag{29}$$

where $\tilde{M}_\pi$ refers to the explicit $M_\pi$-dependence from the pion propagator in the OPE contribution. In order to assess the sensitivity of the triple-alpha process (and of the various energy levels involved in that process) to shifts in $M_\pi$, we will compute quantities of the form $\partial E_i/\partial M_\pi$ at the physical point. Given Eq. (29), we find

$$\begin{aligned}\left.\frac{\partial E_i}{\partial M_\pi}\right|_{M_\pi^{\rm ph}} = {} & \left.\frac{\partial E_i}{\partial \tilde{M}_\pi}\right|_{M_\pi^{\rm ph}} + x_1 \left.\frac{\partial E_i}{\partial m_N}\right|_{m_N^{\rm ph}} + x_2 \left.\frac{\partial E_i}{\partial \tilde{g}_{\pi N}}\right|_{\tilde{g}_{\pi N}^{\rm ph}} \\ & + x_3 \left.\frac{\partial E_i}{\partial C_0}\right|_{C_0^{\rm ph}} + x_4 \left.\frac{\partial E_i}{\partial C_I}\right|_{C_I^{\rm ph}},\end{aligned} \tag{30}$$

where we have introduced the definitions

$$x_3 \equiv \left.\frac{\partial C_0}{\partial M_\pi}\right|_{M_\pi^{\rm ph}}, \quad x_4 \equiv \left.\frac{\partial C_I}{\partial M_\pi}\right|_{M_\pi^{\rm ph}}, \tag{31}$$

for the short-range components of the LO amplitude. Our method for re-expressing the scheme-dependent parameters $x_3$ and $x_4$ in terms of $\bar{A}_s$ and $\bar{A}_t$ is explained in Section 4. The AFQMC calculation of the partial derivatives in Eq. (30) is detailed in Section 5.

## 4 Short-range contributions to the nuclear force

With the exception of the OPE contribution, much of the $M_\pi$-dependence of the nuclear Hamiltonian is implicit and thus controlled by the coefficients $x_i$, which describe how $m_N, \tilde{g}_{\pi N}, C_0$ and $C_I$ depend on $M_\pi$. As discussed in Section 3, $x_1$ and $x_2$ are fairly well constrained by ChPT calculations in combination with lattice QCD data, and provide external input to our analysis according to Eqs. (23) and (27). Contrary to $x_1$ and $x_2$, the coefficients $x_3$ and

$x_4$ are strongly scheme-dependent. We shall therefore express these in terms of the scheme-independent quantities $\bar{A}_s$ and $\bar{A}_t$. This substitution is achieved by an analysis of the two-nucleon scattering problem on a periodic lattice. Once the dependence of the $S$–wave scattering lengths in the spin-singlet and triplet channels on $M_\pi$ is known, $x_3$ and $x_4$ can be straightforwardly obtained.

We use the finite volume formula due to Lüscher [35, 36] which relates the energy levels of a two-body system in a cubic periodic volume of length $L$ to the scattering phase shifts. For the $S$-wave case, we have

$$p \cot \delta = \frac{1}{\pi L} S(\eta) \approx -\frac{1}{a}, \qquad \eta \equiv \left(\frac{pL}{2\pi}\right)^2, \tag{32}$$

where the three-dimensional zeta function $S(\eta)$ is given by

$$S(\eta) = \lim_{\Lambda\to\infty} \left[ \sum_{\boldsymbol{n}} \frac{\theta(\Lambda^2 - \boldsymbol{n}^2)}{\boldsymbol{n}^2 - \eta} - 4\pi\Lambda \right]. \tag{33}$$

For $|\eta| < 1$, it is convenient to expand $S(\eta)$ in powers of $\eta$ as shown in Ref. [37]. We now differentiate Eq. (32) with respect to $M_\pi$, which yields

$$\frac{\partial a^{-1}}{\partial M_\pi} = -\frac{1}{\pi L} S'(\eta) \frac{\partial \eta}{\partial M_\pi}. \tag{34}$$

If we denote the two-nucleon energy in the singlet channel by $E_s$ and that in the triplet channel by $E_t$, we find

$$\frac{\partial \eta_{s,t}}{\partial M_\pi} = \left(\frac{L}{2\pi}\right)^2 \left( E_{s,t} \frac{\partial m_N}{\partial M_\pi} + m_N \frac{\partial E_{s,t}}{\partial M_\pi} \right), \tag{35}$$

and by introducing the notation of Eq. (28), we obtain the relations

$$\begin{aligned} -\zeta_s^{-1} \bar{A}_s = {} & \left.\frac{\partial E_s}{\partial \tilde{M}_\pi}\right|_{M_\pi^{\rm ph}} + x_1 \left( \frac{E_s}{m_N} + \left.\frac{\partial E_s}{\partial m_N}\right|_{m_N^{\rm ph}} \right) \\ & + x_2 \left.\frac{\partial E_s}{\partial \tilde{g}_{\pi N}}\right|_{\tilde{g}_{\pi N}^{\rm ph}} + (x_3 + x_4)\, q_s, \end{aligned} \tag{36}$$

$$\begin{aligned} -\zeta_t^{-1} \bar{A}_t = {} & \left.\frac{\partial E_t}{\partial \tilde{M}_\pi}\right|_{M_\pi^{\rm ph}} + x_1 \left( \frac{E_t}{m_N} + \left.\frac{\partial E_t}{\partial m_N}\right|_{m_N^{\rm ph}} \right) \\ & + x_2 \left.\frac{\partial E_t}{\partial \tilde{g}_{\pi N}}\right|_{\tilde{g}_{\pi N}^{\rm ph}} + (x_3 - 3x_4)\, q_t, \end{aligned} \tag{37}$$

where we have defined

$$\zeta_{s,t} \equiv \frac{m_N L}{4\pi^3} S'(\eta_{s,t}), \qquad q_{s,t} \equiv \left.\frac{\partial E_{s,t}}{\partial C_0}\right|_{C_0^{\rm ph}}. \tag{38}$$

Our results for the energies $E_{s,t}$ and the corresponding partial derivatives, including the factors $q_{s,t}$, are summarized in Table 1. These are computed by exact numerical solution of the two-nucleon problem on a spatial lattice. As the objective is to take the box size $N$ (with $L = Na$) large enough to make finite volume effects negligible, two different box sizes ($N = 24$ and $N = 32$) have been considered in order to determine the magnitude of residual finite volume effects on the Lüscher analysis. Given Eqs. (36) and (37) and the results in Table 1, we are in the position to compute $x_3$ and $x_4$ for use in Eq. (30). However, it is also instructive to eliminate $x_3$ and $x_4$ analytically, which provides an alternative to the parametrization of Eq. (30). This is particularly useful when we express our final results in terms of $\bar{A}_s$ and $\bar{A}_t$, as the current knowledge of these parameters contains sizable uncertainties. Elimination of $x_3$ and $x_4$ in favor of $\bar{A}_s$ and $\bar{A}_t$ gives

**Table 1.** LO energies (in MeV) of the spin-singlet ($E_s$) and spin-triplet ($E_t$) two-nucleon states used in the Lüscher analysis, along with the required partial derivatives. The results were obtained by numerical solution of the Schrödinger equation in a cubic box of size $N = 24$ (second column) and $N = 32$ (third column). $E_d$ denotes the energy of the deuteron. Quantities labeled "[l.u.]" are given in units of the inverse (spatial) lattice spacing. All derivatives are evaluated at the physical point.

| | $L = 47.36$ fm | $L = 63.14$ fm |
|---|---|---|
| $E_s$(LO) [MeV] | $-0.0440956$ | $-0.0218593$ |
| $E_t$(LO) [MeV] | 0.0369820 | 0.0142463 |
| $E_d$(LO) [MeV] | $-2.2244401$ | $-2.2443719$ |
| $\partial E_s/\partial \tilde{M}_\pi$ | $-2.0261727\times10^{-4}$ | $-1.1927443\times10^{-4}$ |
| $\partial E_t/\partial \tilde{M}_\pi$ | $-5.5518808\times10^{-5}$ | $-1.9921726\times10^{-5}$ |
| $\partial E_s/\partial m_N$ | $-2.0081283\times10^{-4}$ | $-1.2224536\times10^{-4}$ |
| $\partial E_t/\partial m_N$ | $-1.6013626\times10^{-4}$ | $-5.8480992\times10^{-5}$ |
| $\partial E_s/\partial \tilde{g}_{\pi N}$[l.u.] | $9.9946261\times10^{-4}$ | $5.8797858\times10^{-4}$ |
| $\partial E_t/\partial \tilde{g}_{\pi N}$[l.u.] | $3.5402207\times10^{-4}$ | $1.2691192\times10^{-4}$ |
| $q_s$ [l.u.] | 0.00379650 | 0.00223108 |
| $q_t$ [l.u.] | 0.00165886 | $5.9467427\times10^{-4}$ |

$$\begin{aligned} \left.\frac{\partial E_i}{\partial M_\pi}\right|_{M_\pi^{\rm ph}} \equiv {} & -\frac{Q_s^{\rm MC}}{\zeta_s} \bar{A}_s - \frac{Q_t^{\rm MC}}{\zeta_t} \bar{A}_t - Q_s^{\rm MC} R_s(x_1, x_2) \\ & - Q_t^{\rm MC} R_t(x_1, x_2) + R_{\rm MC}(x_1, x_2), \end{aligned} \tag{39}$$

which is equivalent to Eq. (30). Here, the notation "MC" indicates which quantities incorporate information from the AFQMC framework. In this parametrization, the individual terms may be obtained using the numbers in Table 1, together with the AFQMC results of Section 5. In Eq. (39), we have introduced the quantities

$$Q_s^{\rm MC} \equiv \frac{3}{4q_s} \left.\frac{\partial E_i}{\partial C_0}\right|_{C_0^{\rm ph}} + \frac{1}{4q_s} \left.\frac{\partial E_i}{\partial C_I}\right|_{C_I^{\rm ph}}, \tag{40}$$

$$Q_t^{\rm MC} \equiv \frac{1}{4q_t} \left.\frac{\partial E_i}{\partial C_0}\right|_{C_I^{\rm ph}} - \frac{1}{4q_t} \left.\frac{\partial E_i}{\partial C_I}\right|_{C_I^{\rm ph}}, \tag{41}$$

for which the error is given entirely by the statistical uncertainty of the AFQMC calculation. We also have

$$R_s(x_1,x_2) \equiv \left.\frac{\partial E_s}{\partial \tilde{M}_\pi}\right|_{M_\pi^{\rm ph}} + x_1 \left(\frac{E_s}{m_N} + \left.\frac{\partial E_s}{\partial m_N}\right|_{m_N^{\rm ph}}\right) + x_2 \left.\frac{\partial E_s}{\partial \tilde{g}_{\pi N}}\right|_{\tilde{g}_{\pi N}^{\rm ph}}, \quad (42)$$

$$R_t(x_1,x_2) \equiv \left.\frac{\partial E_t}{\partial \tilde{M}_\pi}\right|_{M_\pi^{\rm ph}} + x_1 \left(\frac{E_t}{m_N} + \left.\frac{\partial E_t}{\partial m_N}\right|_{m_N^{\rm ph}}\right) + x_2 \left.\frac{\partial E_t}{\partial \tilde{g}_{\pi N}}\right|_{\tilde{g}_{\pi N}^{\rm ph}}, \quad (43)$$

where, in contrast, the dominant sources of uncertainty come from $x_1$ and $x_2$. Finally, we have

$$R_{\rm MC}(x_1,x_2) \equiv \left.\frac{\partial E_i}{\partial \tilde{M}_\pi}\right|_{M_\pi^{\rm ph}} + x_1 \left.\frac{\partial E_i}{\partial m_N}\right|_{m_N^{\rm ph}} + x_2 \left.\frac{\partial E_i}{\partial \tilde{g}_{\pi N}}\right|_{\tilde{g}_{\pi N}^{\rm ph}}, \quad (44)$$

which combines the AFQMC results for the OPE and kinetic energy contributions. The error of $R_{\rm MC}$ receives contributions from the statistical AFQMC error as well as from $x_1$ and $x_2$.

While the most convenient way to obtain our final results is by means of Eq. (39), we may also use the values given in Table 1 to solve Eqs. (36) and (37) for $x_3$ and $x_4$, and to express these as functions of $\bar{A}_{s,t}$ and $x_{1,2}$. This also allows us to illustrate the size of the finite volume effects in the Lüscher analysis. We obtain the relations

$$x_3 = 4.8394\times10^{-2} + 6.7146\times10^{-2}\,x_1 - 0.25080\,x_2 - 0.37540\,\bar{A}_s - 0.20377\,\bar{A}_t, \quad (45)$$

$$x_4 = 4.9754\times10^{-3} - 1.8813\times10^{-3}\,x_1 - 1.2462\times10^{-2}\,x_2 - 0.12513\,\bar{A}_s + 0.20377\,\bar{A}_t, \quad (46)$$

for the smaller $N=24$ lattice ($L=47.36$ fm), and

$$x_3 = 4.8470\times10^{-2} + 6.7127\times10^{-2}\,x_1 - 0.25101\,x_2 - 0.37652\,\bar{A}_s - 0.20467\,\bar{A}_t, \quad (47)$$

$$x_4 = 4.9901\times10^{-3} - 1.8998\times10^{-3}\,x_1 - 1.2532\times10^{-2}\,x_2 - 0.12551\,\bar{A}_s + 0.20467\,\bar{A}_t, \quad (48)$$

for the larger $N=32$ lattice ($L=63.14$ fm). In the above equations, the dimensionful quantities $x_2$, $x_3$ and $x_4$ should be taken in units of the corresponding powers of the inverse lattice spacing. We note that the results for $N=24$ and $N=32$ are practically indistinguishable. In Section 5, we shall make use of the $N=32$ lattice when presenting our final results.

## 5 Auxiliary Field Quantum Monte Carlo results

We now turn to the AFQMC calculation of the shifts in the $E_i$. Our Monte Carlo simulations are performed for a single value of $M_\pi$, equal to the neutral pion mass, with isospin symmetry breaking treated as a perturbation. The partial derivatives $\partial E_i/\partial C_0$ and $\partial E_i/\partial C_I$ are obtained by computing the matrix elements of the associated operators according to Eq. (12). On the other hand, the partial derivatives $\partial E_i/\partial \tilde{M}_\pi$ with respect to the pion mass in the OPE term are computed by evaluating in perturbation theory the energy shift $\Delta E_i$ induced by the substitution $H(\tilde{M}_\pi) \to H(\tilde{M}_\pi + \Delta\tilde{M}_\pi)$ in the nuclear Hamiltonian. Here, the masses of both the neutral and charged pions in the OPE term have been shifted by $\Delta M_\pi = 4.59$ MeV, which equals the empirical mass difference between the neutral and charged pions. The corresponding partial derivatives $\partial E_i/\partial \tilde{M}_\pi$ that enter Eqs. (30) and (44) are then given by

$$\left.\frac{\partial E_i}{\partial \tilde{M}_\pi}\right|_{M_\pi^{\rm ph}} \simeq \frac{\Delta E_i(\Delta\tilde{M}_\pi)}{\Delta M_\pi}, \quad (49)$$

which we find accurate to within the statistical error of the AFQMC calculation. We shall also briefly consider the closely related energy shift $\Delta E_i(\Delta\tilde{M}_\pi^{\rm IB})$, given by the substitution $H(\tilde{M}_\pi) \to H(\tilde{M}_\pi + \Delta\tilde{M}_\pi^{\rm IB})$ in the nuclear Hamiltonian. In this case, only the masses of the charged pions are shifted to their physical value. Finally, the partial derivatives $\partial E_i/\partial \tilde{g}_{\pi N}$ and $\partial E_i/\partial \tilde{m}_N$ are obtained as a finite difference, by defining the quantities $\tilde{g}_{\pi N} \pm \Delta\tilde{g}_{\pi N}$ and $m_N \pm \Delta m_N$, followed by computation of the resulting shifts of the $E_i$ in perturbation theory.

All AFQMC results presented here have been extrapolated to infinite Euclidean time ($N_t = \infty$). Such an extrapolation is necessary, as increasing the number of Euclidean time steps beyond $N_t = 14$ for $^4$He and $N_t = 12$ for the heavier nuclei becomes impractical due to the worsening sign problem. An accurate extrapolation is necessary for reliable conclusions. As an example, on an $N=6$ lattice the calculated $^4$He binding energy at $N_t = 14$ still deviates from the extrapolated value at the $\sim 10\%$ level. The extrapolation of the LO energies $E_i$ is performed using the

**Table 2.** Validation of the extrapolation $N_t \to \infty$ to infinite Euclidean time. The LO deuteron energy $E_d$ and the corresponding energy shifts and derivatives (at the physical point) are computed using AFQMC and extrapolated $N_t \to \infty$ (second column) and compared with the values obtained from the numerical solution of the Schrödinger equation (third column). The appropriate units are given for each quantity, with "[l.u.]" indicating units of the inverse (spatial) lattice spacing. Parentheses indicate one-standard-deviation errors.

| | $^2$H (MC+ex) | $^2$H (exact) |
|---|---|---|
| $E_d$(LO) [MeV] | −9.070(12) | −9.078 |
| $\Delta E_d(\Delta\tilde{M}_\pi)$ [MeV] | −0.003548(12) | −0.003569 |
| $\Delta E_d(\Delta\tilde{M}_\pi^{\rm IB})$ [MeV] | −0.002372(8) | −0.002379 |
| $\partial E_d/\partial m_N$ | −0.00382(2) | −0.003809 |
| $\partial E_d/\partial \tilde{g}_{\pi N}$ [l.u.] | 0.01024(11) | 0.01017 |
| $\partial E_d/\partial C_0$ [l.u.] | 0.13897(15) | 0.138867 |
| $\partial E_d/\partial C_I$ [l.u.] | −0.4171(4) | −0.41660 |

trial function

$$E_i(N_t) = E_i(\infty) + c_{E,i} \exp\left(-\frac{N_t}{\tau_i}\right), \qquad (50)$$

and all matrix elements computed in perturbation theory (energy shifts and partial derivatives, collectively labeled $X_i$) are extrapolated with

$$X_i(N_t) = X_i(\infty) + c_{X,i} \exp\left(-\frac{N_t}{2\tau_i}\right), \qquad (51)$$

using the exponent $\tau_i$ from Eq. (50). The extrapolation is performed by means of a simultaneous chi-square minimization for all quantities, such that the fitted parameters are $E_i(\infty), X_i(\infty), c_{E,i}, c_{X,i}$ and $\tau_i$. The AFQMC data for each nucleus is fitted with a distinct correlation length $\tau_i$. In general, we observe that the rate of convergence with $N_t$ is larger for the $^{12}$C ground and Hoyle states than for $^4$He and $^8$Be.

We have also investigated sources of systematical error that arise from the restriction of the extrapolation to a single exponential $\tau_i$, which is taken to be common for all matrix elements in a given channel. We find that the stability of the single-exponential extrapolations for $^4$He and $^8$Be requires that the data for the matrix elements be excluded for $N_t < 6$, and that $\tau_i$ depends significantly on the choice of trial wave function. We therefore conclude that the single-exponential *ansatz* is more reliable for $^{12}$C. A more accurate extrapolation should allow for multiple exponentials, which may affect each matrix element in a given nuclear channel to a varying extent. In order to reliably perform such an analysis, substantially more AFQMC data is required, including data for multiple trial wave functions. At present, the uncertainties in $\bar{A}_{s,t}$ and $x_{1,2}$ clearly outweigh the additional systematical error introduced by the restriction of the extrapolation to a single exponential $\tau_i$ for each nuclear channel.

We shall first provide an argument for the reliability of our single-exponential description by considering the extrapolation to $N_t = \infty$ for the deuteron. Such a validation of our extrapolation procedure is given in Table 2, where the extrapolated AFQMC results for the deuteron (see Fig. 1) are compared with a direct numerical solution of the Schrödinger equation for an identical Hamiltonian. The AFQMC test results for the deuteron were obtained in a relatively small box size of $L = 5.92$ fm ($N = 3$). The comparison in Table 2 shows excellent agreement between the extrapolated and exact results, which gives confidence that the extrapolation procedure employed in our analysis is indeed reliable. We may then proceed with the AFQMC calculation for the nuclei relevant to the triple-alpha process. The results for $^4$He and $^8$Be are summarized in Table 3, and the individual MC data points along with the extrapolation are shown in Figs. 2 and 3. The results for the ground and Hoyle states of $^{12}$C are similarly given in Table 4 and Fig. 4. These AFQMC calculations were performed on a $L = 11.84$ fm ($N = 6$) lattice, which is large enough to render residual finite volume effects smaller than the expected error from truncation of the chiral expansion of the NN interaction at N$^2$LO.

**Table 3.** AFQMC results for $^4$He and $^8$Be. The LO energies $E_i$ and the corresponding energy shifts (including the EM shifts) and derivatives (at the physical point) have been extrapolated $N_t \to \infty$. The appropriate units are given for each quantity, with "[l.u.]" indicating units of the inverse (spatial) lattice spacing. Parentheses indicate one-standard-deviation errors. All derivatives are computed at the physical point.

| | $^4$He (MC+ex) | $^8$Be (MC+ex) |
|---|---|---|
| $E_i$(LO) [MeV] | −28.89(11) | −57.2(5) |
| $\Delta E_i(\Delta\tilde{M}_\pi)$ [MeV] | −0.2290(17) | −0.477(5) |
| $\Delta E_i(c_{pp})$ [MeV] | 0.433(3) | 1.02(3) |
| $\Delta E_i(\alpha_{\rm em})$ [MeV] | 0.613(2) | 2.35(2) |
| $\partial E_i/\partial m_N$ | −0.0750(7) | −0.187(6) |
| $\partial E_i/\partial \tilde{g}_{\pi N}$ [l.u.] | 0.337(3) | 0.746(12) |
| $\partial E_i/\partial C_0$ [l.u.] | 1.527(12) | 3.52(8) |
| $\partial E_i/\partial C_I$ [l.u.] | −1.881(17) | −4.22(7) |

**Table 4.** AFQMC results for the Hoyle state (second column) and the ground state (third column) of $^{12}$C. The LO energies $E_i$ and the corresponding energy shifts (including the EM shifts) and derivatives (at the physical point) have been extrapolated $N_t \to \infty$. The appropriate units are given for each quantity, with "[l.u.]" indicating units of the inverse (spatial) lattice spacing. Parentheses indicate one-standard-deviation errors. All derivatives are computed at the physical point.

| | $^{12}$C$^\star$(MC+ex) | $^{12}$C (MC+ex) |
|---|---|---|
| $E_i$(LO) [MeV] | −89.8(13) | −95.6(6) |
| $\Delta E_i(\Delta\tilde{M}_\pi)$ [MeV] | −0.802(2) | −0.778(4) |
| $\Delta E_i(c_{pp})$ [MeV] | 2.032(10) | 1.95(2) |
| $\Delta E_i(\alpha_{\rm em})$ [MeV] | 5.54(2) | 5.67(2) |
| $\partial E_i/\partial m_N$ | −0.403(5) | −0.395(5) |
| $\partial E_i/\partial \tilde{g}_{\pi N}$ [l.u.] | 1.343(13) | 1.285(16) |
| $\partial E_i/\partial C_0$ [l.u.] | 6.86(3) | 6.55(7) |
| $\partial E_i/\partial C_I$ [l.u.] | −7.92(3) | −7.54(6) |

We may now combine our AFQMC results with the two-nucleon scattering analysis, in order to obtain predictions for the $M_\pi$-dependence of the various states featuring in the triple-alpha process. This can be performed straightforwardly by substituting the AFQMC results and the numbers from Table 1 into Eq. (39), and by propagating the various sources of error. As described in Section 3, we adopt

$$x_1 = 0.73^{+0.24}_{-0.16}\,, \qquad x_2 = -0.024^{+0.032}_{-0.034}\ \text{l.u.}, \qquad (52)$$

for the central values and uncertainties in $x_1$ and $x_2$, and express the results as a function of $\bar{A}_s$ and $\bar{A}_t$. In this way, we obtain the following results for the $M_\pi$-dependence of

the energy levels involved in the triple-alpha process,

$$\left.\frac{\partial E_4}{\partial M_\pi}\right|_{M_\pi^{\rm ph}} = -\,0.339(5)\,\bar{A}_s - 0.697(4)\,\bar{A}_t + 0.0380(14)^{+0.008}_{-0.006}, \quad (53)$$

$$\left.\frac{\partial E_8}{\partial M_\pi}\right|_{M_\pi^{\rm ph}} = -\,0.794(32)\,\bar{A}_s - 1.584(23)\,\bar{A}_t + 0.089(9)^{+0.017}_{-0.011}, \quad (54)$$

$$\left.\frac{\partial E_{12}}{\partial M_\pi}\right|_{M_\pi^{\rm ph}} = -\,1.52(3)\,\bar{A}_s - 2.88(2)\,\bar{A}_t + 0.159(7)^{+0.023}_{-0.018}, \quad (55)$$

$$\left.\frac{\partial E^\star_{12}}{\partial M_\pi}\right|_{M_\pi^{\rm ph}} = -\,1.588(11)\,\bar{A}_s - 3.025(8)\,\bar{A}_t + 0.178(4)^{+0.026}_{-0.021}, \quad (56)$$

where the error receives contributions both from the statistical error of the AFQMC calculation (given in parentheses) as well as from the uncertainties in $x_1$ and $x_2$ (explicit positive and negative bounds given). It is noteworthy that $x_1$ and $x_2$ only affect the constant terms in the above results, and therefore the (sizable) uncertainties in these coefficients have a relatively minor impact. We can also assess the sensitivity to small shifts in $M_\pi$ by computing the "$K$-factors" as defined in Eq. (14). For this purpose, we take $M_\pi = 138.0$ MeV as the isospin-averaged pion mass, and the empirical values $E_4^{\rm exp} = -28.30$ MeV, $E_8^{\rm exp} = -56.50$ MeV, $E_{12}^{\rm exp} = -92.16$ MeV, and $E_{12}^{\star\rm exp} = -84.51$ MeV for the $E_i$. This yields

$$K^\pi_{E_4} = 1.652(25)\,\bar{A}_s + 3.401(21)\,\bar{A}_t - 0.185(7)^{+0.029}_{-0.039}, \quad (57)$$

$$K^\pi_{E_8} = 1.94(8)\,\bar{A}_s + 3.87(6)\,\bar{A}_t - 0.217(21)^{+0.027}_{-0.041}, \quad (58)$$

$$K^\pi_{E_{12}} = 2.27(4)\,\bar{A}_s + 4.32(3)\,\bar{A}_t - 0.239(11)^{+0.026}_{-0.034}, \quad (59)$$

$$K^\pi_{E^\star_{12}} = 2.593(19)\,\bar{A}_s + 4.940(13)\,\bar{A}_t - 0.291(7)^{+0.034}_{-0.043}, \quad (60)$$

where the same conventions for the errors have been applied. Having calculated the shifts of the individual energy levels involved in the triple-alpha process, we may combine these and obtain similar predictions for the energy differences $\Delta E_b$, $\Delta E_h$ and in particular for $\varepsilon$, which is the critical control parameter for the triple-alpha reaction rate $r_{3\alpha}$ in Eq. (3). We find

$$\left.\frac{\partial \Delta E_b}{\partial M_\pi}\right|_{M_\pi^{\rm ph}} = -\,0.117(34)\,\bar{A}_s - 0.189(24)\,\bar{A}_t + 0.013(9)^{+0.003}_{-0.002}, \quad (61)$$

$$\left.\frac{\partial \Delta E_h}{\partial M_\pi}\right|_{M_\pi^{\rm ph}} = -\,0.455(35)\,\bar{A}_s - 0.744(24)\,\bar{A}_t + 0.051(10)^{+0.008}_{-0.009}, \quad (62)$$

$$\left.\frac{\partial \varepsilon}{\partial M_\pi}\right|_{M_\pi^{\rm ph}} = -\,0.572(19)\,\bar{A}_s - 0.933(15)\,\bar{A}_t + 0.064(6)^{+0.010}_{-0.009}, \quad (63)$$

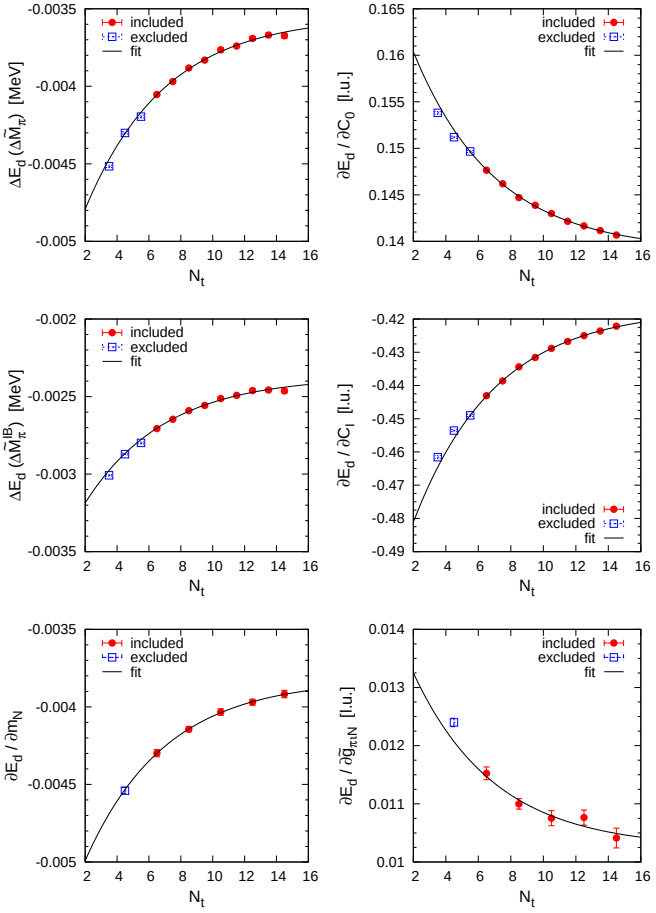



**Fig. 1.** AFQMC calculation of the deuteron, as a function of Euclidean time $N_t$. Results after the extrapolation $N_t \to \infty$ are given in Table 2. The results for $E_d$(LO) have been omitted, as they show no appreciable dependence on $N_t$, and can thus be trivially extrapolated.

and

$$K^\pi_{\Delta E_b} = -175(51)\,\bar{A}_s - 284(36)\,\bar{A}_t + 19(13)^{+4.5}_{-3.0}, \quad (64)$$

$$K^\pi_{\Delta E_h} = -217(16)\,\bar{A}_s - 355(12)\,\bar{A}_t + 25(5)^{+4.0}_{-4.5}, \quad (65)$$

$$K^\pi_{\varepsilon} = -208(7)\,\bar{A}_s - 339(5)\,\bar{A}_t + 23(2)^{+3.7}_{-3.4}, \quad (66)$$

where we have used the empirical values $\Delta E_b^{\rm exp} = 92$ keV, $\Delta E_h^{\rm exp} = 289$ keV, and $\varepsilon = 380$ keV.

We now turn our attention to the AFQMC results for the EM shifts. As explained in Section 2, our objective is to compute the energy shifts $Q_{\rm em}(E_i)$ defined in Eq. (16). This involves the unknown parameter $x_{pp}$, which determines the relative strength of the proton-proton contact interaction that emerges from the lattice regularization of the long-range Coulomb force. We may fix $x_{pp}$ by means of the known contribution of the Coulomb force to the binding energy of $^4$He, which is $Q_{\rm em}(E_4) = 0.78(3)$ MeV [38]. The quoted error reflects the model-dependence and is determined from the range of values corresponding to different phenomenological two- and three-nucleon potentials as well as nuclear forces derived in chiral EFT. Using the

AFQMC results for $\Delta E_i(\alpha_{\rm em})$ and $\Delta E_i(c_{pp})$ from Table 3, we find

$$\begin{aligned} Q_{\rm em}(E_4) &= 0.433(3)\ \text{MeV} \times x_{pp} + 0.613(2)\ \text{MeV} \\ &\stackrel{!}{=} 0.78(3)\ \text{MeV} \ \ \rightarrow \ \ x_{pp} \simeq 0.39(5), \end{aligned} \tag{67}$$

for $^4$He, which enables us to predict

$$\begin{aligned} Q_{\rm em}(E_8) &= 1.02(3)\ \text{MeV} \times x_{pp} + 2.35(2)\ \text{MeV} \\ &= 2.75(8)\ \text{MeV}, \end{aligned} \tag{68}$$

for $^8$Be. Further, using the value $x_{pp} = 0.39(5)$ and the AFQMC results given in Table 4, we predict

$$\begin{aligned} Q_{\rm em}(E_{12}^\star) &= 2.032(10)\ \text{MeV} \times x_{pp} + 5.54(2)\ \text{MeV} \\ &= 6.33(6)\ \text{MeV}, \end{aligned} \tag{69}$$

for the Hoyle state, and

$$\begin{aligned} Q_{\rm em}(E_{12}) &= 1.95(2)\ \text{MeV} \times x_{pp} + 5.67(2)\ \text{MeV} \\ &= 6.43(6)\ \text{MeV}, \end{aligned} \tag{70}$$

for the ground state of $^{12}$C. We are now in the position to predict the EM shifts of the energy differences $\Delta E_b$, $\Delta E_h$ and $\varepsilon$. This gives

$$\begin{aligned} Q_{\rm em}(\Delta E_h) &= 2.80(10)\ \text{MeV}, \\ Q_{\rm em}(\Delta E_b) &= 1.19(8)\ \text{MeV}, \\ Q_{\rm em}(\varepsilon) &= 3.99(9)\ \text{MeV}. \end{aligned} \tag{71}$$

We have also studied the dependence of the excitation energy $\Delta E_c$ of the Hoyle state on $M_\pi$ and $\alpha_{\rm em}$. Although $\Delta E_c$ is not needed for the calculation of the triple-alpha reaction rate, it provides an instructive reference point when discussing the sensitivity of various energy differences to small changes in the fundamental constants. We compute $\Delta E_c$ from

$$\Delta E_c \equiv E_{12}^\star - E_{12}, \tag{72}$$

for which we find

$$\begin{aligned} \left.\frac{\partial \Delta E_c}{\partial M_\pi}\right|_{M_\pi^{\rm ph}} &= -\,0.07(3)\,\bar{A}_s - 0.14(2)\,\bar{A}_t \\ &\quad + 0.019(9)^{+0.004}_{-0.003}\,. \end{aligned} \tag{73}$$

This yields

$$K^\pi_{\Delta E_c} = -1.3(5)\,\bar{A}_s - 2.6(4)\,\bar{A}_t + 0.34(15)^{+0.07}_{-0.05}\,, \tag{74}$$

for the sensitivity to small changes in $M_\pi$. The above result corresponds to the empirical value of $\Delta E_c^{\rm exp} = 7.65$ MeV. Finally, we find

$$Q_{\rm em}(\Delta E_c) = 0.10(7)\ \text{MeV}, \tag{75}$$

for the EM shift in the excitation energy of the Hoyle state.

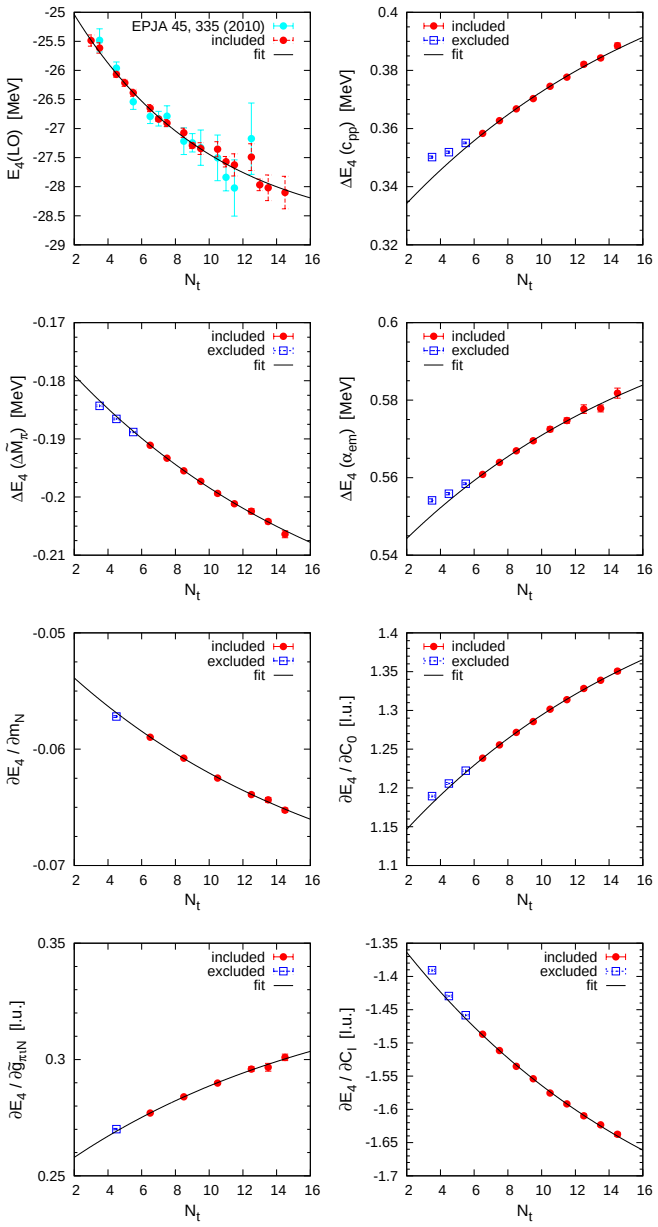



**Fig. 2.** AFQMC calculation of $^4$He, as a function of Euclidean time steps $N_t$. Results after extrapolation $N_t \to \infty$ are given in Table 3. The results of Ref. [19] for $E_4$(LO) are included to highlight the improved statistics, and as a consistency check.

## 6 Theoretical uncertainties and higher-order corrections

In order to estimate the theoretical uncertainty of our results, we shall first consider the effects of neglected higher-order terms in the chiral EFT expansion. To this end, we compute the $M_\pi$-dependence of the $^4$He binding energy induced by the explicitly $M_\pi$-dependent part of the three-

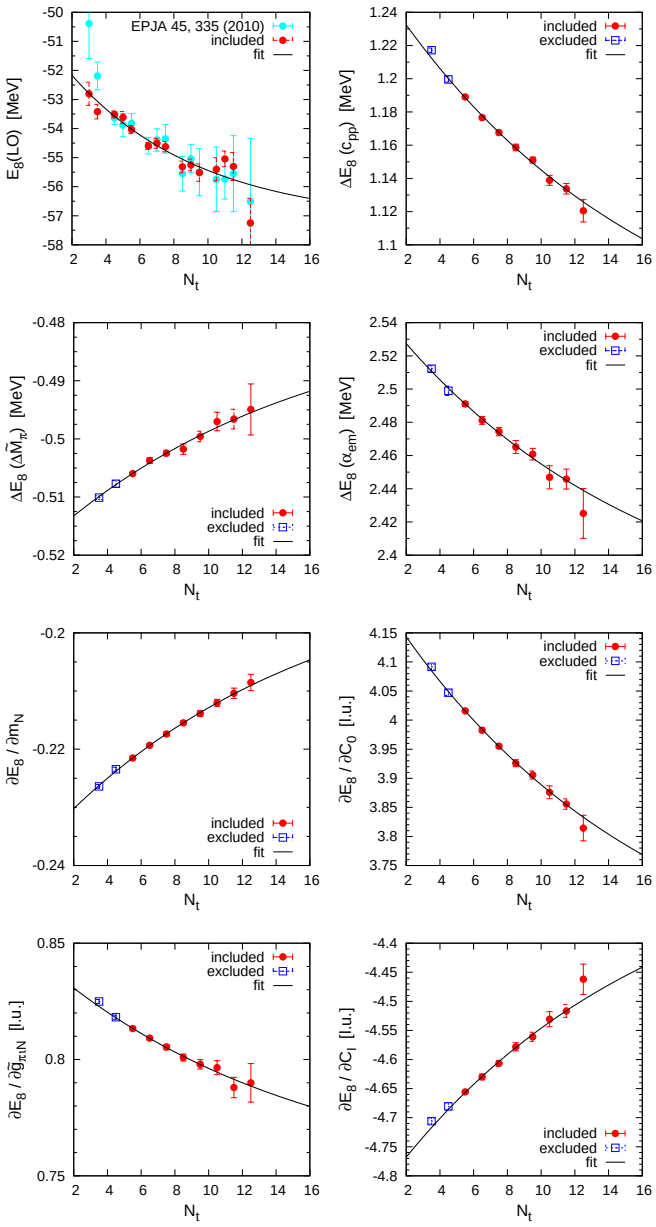



**Fig. 3.** AFQMC calculation of $^8$Be, as a function of Euclidean time steps $N_t$. Results after extrapolation $N_t \to \infty$ are given in Table 3. The results of Ref. [19] for $E_8$(LO) are included to highlight the improved statistics, and as a consistency check.

nucleon force (3NF),

$$\mathcal{A}^{\rm 3NF}_{\rm N^2LO} = \frac{g_A^2}{8F_\pi^4}\,\frac{\boldsymbol{q}_i\cdot\boldsymbol{\sigma}_i\,\boldsymbol{q}_j\cdot\boldsymbol{\sigma}_j}{(\boldsymbol{q}_i^2+M_\pi^2)(\boldsymbol{q}_j^2+M_\pi^2)}\Big[\boldsymbol{\tau}_i\cdot\boldsymbol{\tau}_j\,(-4c_1M_\pi^2 + 2c_3\,\boldsymbol{q}_i\cdot\boldsymbol{q}_j) + c_4(\boldsymbol{\tau}_i\times\boldsymbol{\tau}_j)\cdot\boldsymbol{\tau}_k\,(\boldsymbol{q}_i\times\boldsymbol{q}_j)\cdot\boldsymbol{q}_k\Big] - \frac{g_A D}{8F_\pi^2}\,\frac{\boldsymbol{q}_i\cdot\boldsymbol{\sigma}_i\,\boldsymbol{q}_i\cdot\boldsymbol{\sigma}_j\,\boldsymbol{\tau}_i\cdot\boldsymbol{\tau}_j}{\boldsymbol{q}_i^2+M_\pi^2} + \frac{E}{2}\,\boldsymbol{\tau}_i\cdot\boldsymbol{\tau}_j + \text{permutations}, \tag{76}$$

which contributes at N$^2$LO. For the LECs $c_i$, we take $c_1 = -0.81$ GeV$^{-1}$, $c_3 = -4.7$ GeV$^{-1}$, and $c_4 = 3.4$ GeV$^{-1}$, as determined from low-energy pion-nucleon scattering [39, 40]. The LECs $D$ and $E$ are fixed by means of the triton binding energy and the weak axial vector current. For more details on the treatment of the 3NF in the nuclear lattice simulations, see Ref. [17].

It should be understood that the $M_\pi$-dependence of the $E_i$ induced by that of the 3NF is beyond the accuracy of our analysis. The following estimate of its impact on $E_4$ is only intended as a consistency check. We calculate the sensitivity of $E_4$ to changes in $M_\pi$ entering the 3NF by performing AFQMC calculations using a slightly shifted pion mass in Eq. (76), namely $\tilde M_\pi = M_\pi^{\rm ph} \pm 20$ MeV. The resulting shifts in $E_4$ induced by the 3NF are

$$\begin{aligned} \Delta E_4^{\rm 3NF}\big|_{\tilde M_\pi = M_\pi^{\rm ph}+20\ \rm MeV} &= -3.034(12)\ \text{MeV}, \\ \Delta E_4^{\rm 3NF}\big|_{\tilde M_\pi = M_\pi^{\rm ph}-20\ \rm MeV} &= -3.204(16)\ \text{MeV}, \end{aligned} \tag{77}$$

which gives us the rough estimate

$$\left.\frac{\partial E_4^{\rm 3NF}}{\partial \tilde M_\pi}\right|_{M_\pi^{\rm ph}} \simeq 0.004\ . \tag{78}$$

This is an order of magnitude smaller than e.g. the LO contribution $\partial E_4/\partial \tilde M_\pi|_{M_\pi^{\rm ph}} \simeq -0.05$. This observation suggests that the 3NF effects are indeed very much suppressed, as expected for a N$^2$LO contribution.

It is also instructive to compare our results with the ones of Ref. [52], which were obtained within the framework of *pionless* EFT. Not only does this provide a useful consistency check for our calculations, but it also allows us to estimate our theoretical uncertainty in a complementary way. In particular, we can compare our result for $\partial E_4/\partial M_\pi$ in Eq. (53) with the result for the $^4$He binding energy $B_4$ ($B_i \equiv |B_i| = -E_i$) given in Eqs. (1.5)-(1.7) of Ref. [52]

$$\frac{\partial B_4}{\partial m_q} \simeq 0.037\,\frac{B_4}{a_s}\frac{\partial a_s}{\partial m_q} + 0.74\,\frac{B_4}{B_d}\frac{\partial B_d}{\partial m_q}, \tag{79}$$

where $B_d$ is the deuteron binding energy. Noting that $\partial/\partial m_q \propto \partial/\partial M_\pi$ and making use of the relation

$$\frac{\partial a_s}{\partial M_\pi} = -a_s^2\,\frac{\partial a_s^{-1}}{\partial M_\pi}, \tag{80}$$

we can bring Eq. (79) into the form

$$\frac{\partial B_4}{\partial M_\pi} \simeq -0.037\,B_4 a_s\frac{\partial a_s^{-1}}{\partial m_q} + 0.74\,\frac{B_4}{B_d}\frac{\partial B_d}{\partial M_\pi}, \tag{81}$$

where it is still necessary to convert the dependence on $B_d$ into a corresponding dependence on $a_t$. To this end, we use the effective range approximation

$$p\cot\delta_t \simeq -\frac{1}{a_t} + \frac{1}{2}\,p^2 r_t, \tag{82}$$

to obtain

$$\frac{\partial B_d}{\partial M_\pi} \simeq \frac{4}{m_N[a_t + \sqrt{a_t(a_t-2r_t)} - 2r_t]}\,\frac{\partial a_t^{-1}}{\partial M_\pi} \simeq 0.164\,\frac{\partial a_t^{-1}}{\partial M_\pi}, \tag{83}$$

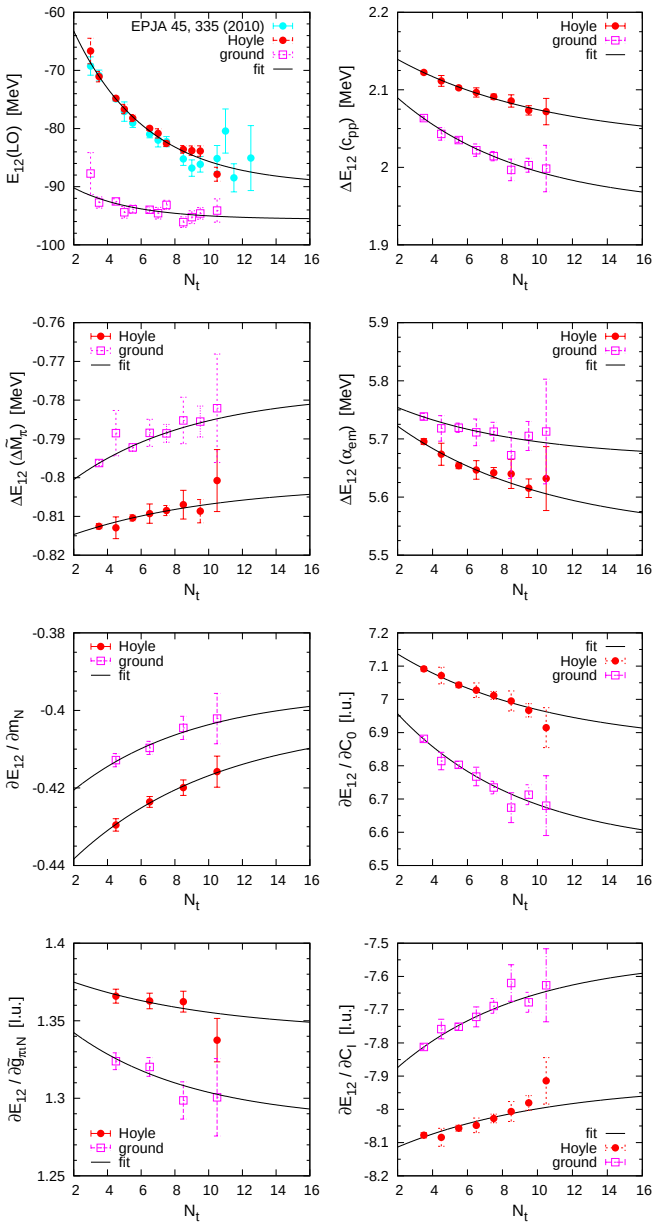



**Fig. 4.** AFQMC calculation of $^{12}$C, as a function of Euclidean time steps $N_t$. Results after extrapolation $N_t \to \infty$ are given in Table 4. The results of Ref. [19] for $E_{12}^{\star}$(LO) are included to highlight the improved statistics, and as a consistency check.

where we have inserted the empirical values $a_t = 5.42$ fm and $r_t = 1.75$ fm. Finally, by combining this expression with Eq. (81) and noting that $B_i = -E_i$, the pionless EFT result of Ref. [52] is brought into the form

$$\left.\frac{\partial E_4}{\partial M_\pi}\right|_{M_\pi^{\rm ph}} \simeq -0.037\, E_4 a_s \bar{A}_s - 1.48\, \frac{E_4}{E_d m_N a_t}\, \bar{A}_t \simeq -0.126\, \bar{A}_s - 0.739\, \bar{A}_t, \qquad (84)$$

which is in a reasonable agreement with Eq. (53). By taking the central values of the coefficients $x_1$ and $x_2$ in Eq. (53), as well as $\bar{A}_s = 0.29$ and $\bar{A}_t = -0.18$ as found in the most recent chiral EFT calculations (see Section 8 for details), we obtain $\partial E_4/\partial M_\pi \simeq 0.065$. This should be compared with the pionless EFT result $\partial E_4/\partial M_\pi \simeq 0.096$ based on Eq. (84). We expect that the theoretical uncertainty of our calculation is much smaller than the difference between these two numbers or, more generally, than the difference between Eqs. (84) and (53). This is because in our approach, the uncertainty is entirely due to suppressed higher order corrections.

Finally, we note that our analysis does not account for the $M_\pi$-dependence of the momentum-dependent, subleading contact interactions in the chiral EFT Hamiltonian. Assuming validity of the naive dimensional analysis, such effects are beyond the accuracy of our present work. In addition, the strong correlations we observe for the $M_\pi$-dependence of the various observables (as discussed in Section 7) indicate that the relevant dynamics is largely governed by the large $S$–wave NN scattering lengths. Higher-order $M_\pi$-dependent short-range terms are therefore expected to play a lesser role.

## 7 Correlations and the binding energy of the alpha particle

Given the results in Section 5, we are now in a position to draw conclusions concerning the individual energies $E_i$ and the associated energy differences. The first interesting observation is that the energy differences $\Delta E_h$, $\Delta E_b$ and $\varepsilon$ are, by themselves, extremely sensitive to changes in $M_\pi$ as could be expected. Such a conclusion follows from the unnaturally large coefficients in Eqs. (64)-(66). Notice that the fact that $\Delta E_h$, $\Delta E_b$ and $\varepsilon$ are much smaller than the individual $E_i$ does not, by itself, imply a strong fine-tuning. For example, the sensitivity of the Hoyle state excitation energy $\Delta E_c$ in Eq. (74) is of a natural size, in spite of $\Delta E_c^{\rm exp} = 7.65$ MeV being almost an order of magnitude smaller than $|E_{12}^{\rm exp}| = 92.16$ MeV.

While we find that $\Delta E_h$, $\Delta E_b$ and $\varepsilon$ are by themselves extremely sensitive to variations in $M_\pi$, we also observe the approximate relations

$$\frac{K^\pi_{\Delta E_h}}{K^\pi_{\Delta E_b}} \simeq 1.25, \qquad \frac{K^\pi_{\Delta E_h}}{K^\pi_{\varepsilon}} \simeq 1.05, \qquad (85)$$

which are satisfied for the central values of the individual terms in Eqs. (64)-(66) at the level of a few percent. This suggests that $\Delta E_h$, $\Delta E_b$ and $\varepsilon$ cannot be independently varied (or fine-tuned) by changing the singlet and triplet NN scattering lengths (or, equivalently, by changing the strength of the short-range NN force in the $^1S_0$ and $^3S_1$ channels). Moreover, it is apparent from Eqs. (57)-(60) that also the energies $E_i$ of the individual states are as well strongly correlated in a similar manner.

In order to quantify and illustrate the observed correlations, we show in Fig. 5 the changes in the sensitivities of $E_8$, $E_{12}$, $E_{12}^{\star}$ and $\Delta E_c$ as a function of $K^\pi_{E_4}$, when $\bar{A}_s$ and $\bar{A}_t$ are independently varied over a large range. The correlations for $\Delta E_h$, $\Delta E_b$ and $\varepsilon$ are shown in a similar way in Fig. 6. Within the statistical accuracy of our AFQMC

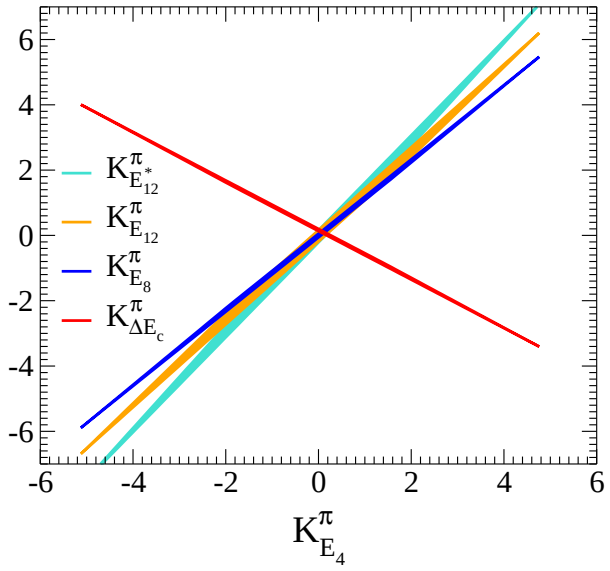



**Fig. 5.** Sensitivities of $E_8$, $E_{12}$, $E^{\star}_{12}$ and $\Delta E_c$ to changes in $M_\pi$, as a function of $K^{\pi}_{E_4}$ under independent variation of $\bar{A}_s$ and $\bar{A}_t$ over the range $\{-1\ldots 1\}$. The bands correspond to $E^{\star}_{12}$, $E_{12}$, $E_8$ and $\Delta E_c$ in clockwise order.

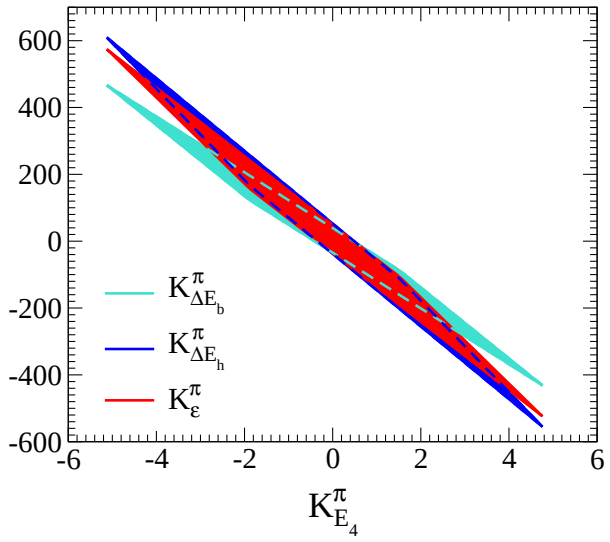



**Fig. 6.** Sensitivities of $\Delta E_h$, $\Delta E_b$ and $\varepsilon$ to changes in $M_\pi$, as a function of $K^{\pi}_{E_4}$ under independent variation of $\bar{A}_s$ and $\bar{A}_t$ over the range $\{-1\ldots 1\}$. The bands correspond to $\Delta E_b$, $\varepsilon$ and $\Delta E_h$ in clockwise order.

results, we may conclude that the scenario of independent variations of the energy levels pertinent to the triple-alpha process under changes in the fundamental parameters is strongly disfavored. Given the prominent role of the $^4$He binding energy in the correlations, the observed behavior is strongly suggestive of the $\alpha$-cluster structure of the $^8$Be, $^{12}$C and Hoyle states. Such correlations related to the production of carbon have indeed been speculated upon earlier [10,14].

## 8 Reaction rate of the triple-alpha process

We now turn our attention to the reaction rate of the triple-alpha process as given by Eq. (3), and determine the range of variations in $m_q$ and $\alpha_{\rm em}$ compatible with the formation of significant amounts of carbon and oxygen in our Universe, and thus with the existence of carbon-oxygen based life. We recall that the stellar modeling calculations of Refs. [13,24] suggest that sufficient abundances of both carbon and oxygen can be maintained within an envelope of $\pm 100$ keV around the empirical value of $\varepsilon = 379.47(18)$ keV. For small variations $|\delta\alpha_{\rm em}/\alpha_{\rm em}| \ll 1$ and $|\delta m_q/m_q| \ll 1$, the resulting change in $\varepsilon$ can be expressed as

$$\begin{aligned}\delta(\varepsilon) &\approx \left.\frac{\partial\varepsilon}{\partial M_\pi}\right|_{M_\pi^{\rm ph}} \delta M_\pi + \left.\frac{\partial\varepsilon}{\partial\alpha_{\rm em}}\right|_{\alpha_{\rm em}^{\rm ph}} \delta\alpha_{\rm em} \\ &= \left.\frac{\partial\varepsilon}{\partial M_\pi}\right|_{M_\pi^{\rm ph}} K^q_{M_\pi} M_\pi \left(\frac{\delta m_q}{m_q}\right) + Q_{\rm em}(\varepsilon)\left(\frac{\delta\alpha_{\rm em}}{\alpha_{\rm em}}\right),\end{aligned} \tag{86}$$

where we recall that $K^q_{M_\pi} = 0.494^{+0.009}_{-0.013}$ [28]. Thus, the condition $|\delta(\varepsilon)| < 100$ keV together with Eq. (71) leads to the predicted tolerance $|\delta\alpha_{\rm em}/\alpha_{\rm em}| \simeq 2.5\%$ of carbon-oxygen based life to shifts in $\alpha_{\rm em}$. This result is compatible with the $\simeq 4\%$ bound reported in Ref. [12]. For shifts in $m_q$, we find

$$\begin{aligned}&\left|\Big[0.572(19)\,\bar{A}_s + 0.933(15)\,\bar{A}_t - 0.064(6)\Big]\left(\frac{\delta m_q}{m_q}\right)\right| \\ &< 0.15\%,\end{aligned} \tag{87}$$

using Eq. (63), where we have neglected the relatively insignificant errors introduced by $x_1$ and $x_2$. The resulting constraints on the values of $\bar{A}_s$ and $\bar{A}_t$ compatible with the condition $|\delta(\varepsilon)| < 100$ keV are visualized in Fig. 7. The various shaded bands in Fig. 7 cover the values of $\bar{A}_s$ and $\bar{A}_t$ consistent with carbon-oxygen based life, when $m_q$ is varied by 0.5%, 1% and 5%.

In the most generic scenario, assuming that both of the dimensionless quantities $\bar{A}_s$ and $\bar{A}_t$ are $\sim \mathcal{O}(1)$, and therefore $0.572(19)\,\bar{A}_s + 0.933(15)\,\bar{A}_t \sim \mathcal{O}(1)$, our results imply that a change in $m_q$ of as little as $\simeq 0.15\%$ would suffice to render carbon-oxygen based life unlikely to exist. Stated differently, the "survivability band" corresponding to $|\delta m_q/m_q| < 0.15\%$ would cover the whole of Fig. 7. It should be noted that in such a generic scenario, one can approximate

$$\left.\frac{\partial\varepsilon}{\partial M_\pi}\right|_{M_\pi^{\rm ph}} \approx 1.5 \left.\frac{\partial E_4}{\partial M_\pi}\right|_{M_\pi^{\rm ph}}, \tag{88}$$

which implies that the binding energy of $^4$He should be fine-tuned under variation of $m_q$ to its empirical value at the level of $\simeq 0.25\%$ in order to fulfill the condition $|\delta(\varepsilon)| < 100$ keV. Nevertheless, there clearly also exists a special value for the ratio of $\bar{A}_s$ to $\bar{A}_t$, given by

$$\bar{A}_s/\bar{A}_t \simeq -1.5, \tag{89}$$

for which the dependence of $\Delta E_h$, $\Delta E_b$ and $\varepsilon$ on $M_\pi$ becomes vanishingly small (compared to the statistical uncertainties of the AFQMC calculation), such that the factor

$$0.572(19)\,\bar{A}_s + 0.933(15)\,\bar{A}_t - 0.064(6) \ll 1, \qquad (90)$$

in Eq. (87). In this case, we would conclude that the reaction rate of the triple-alpha process were completely insensitive to shifts in $m_q$. As the realistic scenario is likely to be found somewhere in between these extreme cases, it becomes important to consider the available constraints on $\bar{A}_s$ and $\bar{A}_t$ before final conclusions are drawn.

The quark mass dependence of the $S$–wave NN scattering lengths has been analyzed within the framework of chiral EFT by several groups. The problem common to these calculations is the lack of knowledge about the $m_q$-dependence of the NN contact interactions. Estimating the size of the corresponding LECs by means of dimensional analysis typically leads to large uncertainties for chiral extrapolations of the scattering lengths. For example, the NLO calculation of Refs. [41,42] resulted in the values

$$K^q_{a_s} = 5 \pm 5, \qquad K^q_{a_t} = 1.1 \pm 0.9, \qquad (91)$$

for the relevant $K$–factors. These are consistent with the NLO analysis of Ref. [43], which yielded

$$K^q_{a_s} = 2.4 \pm 3.0, \qquad K^q_{a_t} = 3.0 \pm 3.5, \qquad (92)$$

based on a perturbative treatment of OPE (see Ref. [45] for a related study). More recently, attempts have been made to combine chiral EFT with lattice QCD calculations. In particular, the NPLQCD collaboration has determined the regions for the $S$–wave scattering lengths consistent with their lattice results, $a_s = (0.63 \pm 0.50)$ fm and $a_t = (0.63 \pm 0.74)$ fm, obtained for $M_\pi = 353.7 \pm 2.1$ MeV [44]. By using these lattice data in conjunction with the assumptions of perturbativeness of the OPE potential in the ${}^3S_1$–${}^3D_1$ channel and validity of the chiral expansion for NN scattering for $M_\pi > 350$ MeV, Refs. [46, 47] obtained results for $K^q_{a_s}$ and $K^q_{a_t}$ which are consistent with the ones quoted in Eq. (91), and in slight disagreement with those of Eq. (92).

Very recently, the analysis of the $m_q$-dependence of NN observables was extended to N$^2$LO in chiral EFT [28]. To overcome the difficulties due to the poorly known $m_q$-dependence of the short-range NN interactions, the authors of Ref. [28] exploited the fact that the LECs accompanying the NN contact interactions are saturated by exchanges of heavy mesons [48]. By means of a unitarized version of ChPT in combination with lattice QCD results, which describes the $m_q$-dependence of the meson resonances saturating these LECs, the $m_q$-dependence of the NN observables was analyzed at N$^2$LO without relying on the chiral expansion of the NN contact interactions. The most up-to-date values are then given by

$$K^q_{a_s} = 2.3^{+1.9}_{-1.8}, \qquad K^q_{a_t} = 0.32^{+0.17}_{-0.18}, \qquad (93)$$

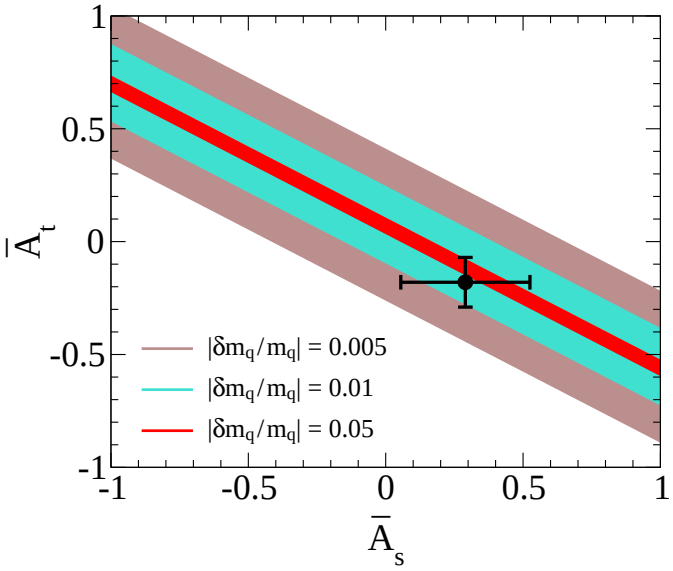



**Fig. 7.** "Survivability bands" for carbon-oxygen based life from Eq. (87), due to 0.5% (broad outer band), 1% (medium band) and 5% (narrow inner band) changes in $m_q$ in terms of the input parameters $\bar{A}_s$ and $\bar{A}_t$. The most up-to-date N$^2$LO analysis of $\bar{A}_s$ and $\bar{A}_t$ corresponding to Eq. (94) is given by the data point with horizontal and vertical error bars.

and

$$\bar{A}_s = -\frac{1}{a_s M_\pi}\frac{K^q_{a_s}}{K^q_{M_\pi}} \simeq 0.29^{+0.25}_{-0.23},$$
$$\bar{A}_t = -\frac{1}{a_t M_\pi}\frac{K^q_{a_t}}{K^q_{M_\pi}} \simeq -0.18^{+0.10}_{-0.10}, \qquad (94)$$

which are not only consistent with the earlier determinations, but also in reasonably good agreement with the (parameter-free) LO chiral EFT calculation of Ref. [49], which is based on a novel, cutoff-independent approach. Interestingly, direct application of the central values in Eq. (94) gives $\bar{A}_s/\bar{A}_t \simeq -1.6$, which leads to a strong cancellation of the dependence of $\Delta E_h$, $\Delta E_b$ and $\varepsilon$ on $\bar{A}_s$ and $\bar{A}_t$, and hence also to a mild dependence on $M_\pi$. The range of values given in Eq. (94) suggests that all contributions to the $K$–factors (notably including $K^\pi_{\Delta E_c}$) are of $\sim \mathcal{O}(1)$, with the exceptions of $K^\pi_{\Delta E_b}$, $K^\pi_{\Delta E_h}$ and $K^\pi_\varepsilon$.

## 9 Summary and conclusions

We may summarize our findings by a brief discussion of Fig. 7, where we have superimposed the result corresponding to Eq. (94) with the "survivability bands" from our AFQMC results in Eq. (87). Given the current theoretical uncertainty in $\bar{A}_s$ and $\bar{A}_t$, our results remain compatible with a vanishing $\partial\varepsilon/\partial M_\pi$, in other words with a complete lack of fine-tuning. Interestingly, Fig. 7 also indicates that the triple-alpha process is unlikely to be fine-tuned to a higher degree than $\simeq 0.8\%$ under variation of $m_q$. The central values of $\bar{A}_s$ and $\bar{A}_t$ from Eq. (94) suggest that variations in the light quark masses of up to $2-3\%$ are unlikely

to be catastrophic to the formation of life-essential carbon and oxygen. A similar calculation of the tolerance for shifts in the EM fine-structure constant $\alpha_{\rm em}$ suggests that carbon-oxygen based life can withstand shifts of $\simeq 2.5\%$ in $\alpha_{\rm em}$. Beyond such relatively small changes in the fundamental parameters, the anthropic principle appears necessary to explain the observed abundances of $^{12}$C and $^{16}$O. We also note that the fine-tuning in the fundamental parameters is much more severe than the one in the energy difference $\varepsilon$.

Our *ab initio* lattice calculations account for all sources of quark mass dependence (explicit as well as implicit) in the LO nuclear Hamiltonian in chiral EFT, although we have not performed a strict LO analysis of the triple-alpha reaction rate. We have considered the potential impact of neglected higher-order terms on our results, in particular that of the 3NF which starts contributing at N$^2$LO in the chiral expansion, and found that our conclusions are likely to be robust against such effects. Therefore, the most immediately useful extension of our work would be the incorporation of a more precise determination of $\bar{A}_s$ and $\bar{A}_t$ from future lattice QCD studies.

As a longer-term objective, we may envision the inclusion of dynamical photons in our AFQMC framework. Such a coupling of lattice QED to lattice chiral EFT may provide a more fundamental understanding of the sensitivity of the triple-alpha process to shifts in $\alpha_{\rm em}$.

## Acknowledgments

We are grateful to Silas Beane and Martin Savage for useful comments. We thank Andreas Nogga for an updated analysis of the $^4$He nucleus. Partial financial support from Deutsche Forschungsgemeinschaft and NSFC (Sino-German CRC 110), Helmholtz Association (contract VH-VI-417), BMBF (grant 06BN9006), and U.S. Department of Energy (DE-FG02-03ER41260) is acknowledged. This work was further supported by the EU HadronPhysics3 project, and by funds provided by the ERC project 259218 NUCLEAREFT. Computational resources for this project were provided by the Jülich Supercomputing Centre (JSC) at the Forschungszentrum Jülich and by RWTH Aachen.

## References

1. F. Hoyle, Astrophys. J. Suppl. Ser. **1**, 121 (1954).
2. D. N. F. Dunbar, R. E. Pixley, W. A. Wenzel, and W. Whaling, Phys. Rev. **92**, 649 (1953).
3. C. W. Cook, W. A. Fowler, C. C. Lauritsen, and T. Lauritsen, Phys. Rev. **107**, 508 (1957).
4. A. Linde, "The inflationary multiverse," in *Universe or multiverse?*, edited by B. Carr (Cambridge University Press, Cambridge, England, 2007).
5. H. Kragh, Arch. Hist. Exact Sci. **64**, 721 (2010).
6. B. Carter, "Large number coincidences and the anthropic principle", in *Confrontation of cosmological theories with observational data*, edited by M. S. Longair (Reidel, Dordrecht, 1974).
7. B. J. Carr and M. Rees, Nature **278**, 605 (1979).
8. S. Weinberg, Phys. Rev. Lett. **59**, 2607 (1987).
9. L. Susskind, "The anthropic landscape of string theory," in *Universe or multiverse?*, edited by B. Carr (Cambridge University Press, Cambridge, England, 2007).
10. M. Livio, D. Hollowell, A. Weiss, and J. W. Truran, Nature **340**, 281 (1989).
11. H. Schlattl, A. Heger, H. Oberhummer, T. Rauscher, and A. Csótó, Astrophys. Space Sci. **291**, 27 (2004).
12. H. Oberhummer, A. Csótó, and H. Schlattl, Nucl. Phys. A **689**, 269 (2001).
13. H. Oberhummer, A. Csótó, and H. Schlattl, Science **289**, 88 (2000).
14. S. Weinberg, "Facing Up" (Harvard University Press, Cambridge, Massachusetts, 2001).
15. B. Borasoy, E. Epelbaum, H. Krebs, D. Lee, and U.-G. Meißner, Eur. Phys. J. A **31**, 105 (2007).
16. D. Lee, Prog. Part. Nucl. Phys. **63**, 117 (2009).
17. E. Epelbaum, H. Krebs, D. Lee, and U.-G. Meißner, Eur. Phys. J. A **41**, 125 (2009).
18. E. Epelbaum, H. Krebs, D. Lee, and U.-G. Meißner, Phys. Rev. Lett. **104**, 142501 (2010).
19. E. Epelbaum, H. Krebs, D. Lee, and U.-G. Meißner, Eur. Phys. J. A **45**, 335 (2010).
20. E. Epelbaum, H. Krebs, D. Lee, and U.-G. Meißner, Phys. Rev. Lett. **106**, 192501 (2011).
21. E. Epelbaum, H. Krebs, D. Lee, and U.-G. Meißner, Eur. Phys. J. A **40**, 199 (2009).
22. E. Epelbaum, H. Krebs, T. A. Lähde, D. Lee, and U.-G. Meißner, Phys. Rev. Lett. **109**, 252501 (2012).
23. E. Epelbaum, H. Krebs, T. A. Lähde, D. Lee, and U.-G. Meißner, Phys. Rev. Lett. **110**, 112502 (2013).
24. H. Oberhummer, A. Csótó, and H. Schlattl, arXiv:astro-ph/9908247.
25. S. Weinberg, Phys. Lett. B **251**, 288 (1990).
26. E. Epelbaum, H.-W. Hammer, and U.-G. Meißner, Rev. Mod. Phys. **81**, 1773 (2009).
27. R. Machleidt and D. R. Entem, Phys. Rept. **503**, 1 (2011).
28. J. C. Berengut, E. Epelbaum, V. V. Flambaum, C. Hanhart, U.-G. Meißner, J. Nebreda, and J. R. Peláez, Phys. Rev. D **87**, 085018 (2013).
29. M. Procura, B. U. Musch, T. Wollenweber, T. R. Hemmert, and W. Weise, Phys. Rev. D **73**, 114510 (2006).
30. V. Bernard, Prog. Part. Nucl. Phys. **60**, 82 (2008).
31. G. Colangelo and S. Dürr, Eur. Phys. J. C **33**, 543 (2004).
32. J. Gasser and H. Leutwyler, Ann. Phys. **158**, 142 (1984).
33. R. Baron, P. Boucaud, J. Carbonell, A. Deuzeman, V. Drach, F. Farchioni, V. Gimenez and G. Herdoiza *et al.*, JHEP **1006**, 111 (2010)
34. V. Bernard and U.-G. Meißner, Phys. Lett. B **639**, 278 (2006).
35. M. Lüscher, Commun. Math. Phys. **105**, 153 (1986).
36. M. Lüscher, Nucl. Phys. B **354**, 531 (1991).
37. D. Lee, Eur. Phys. J. A **35**, 171 (2008).
38. A. Nogga, *private communication.*
39. V. Bernard, N. Kaiser, and U.-G. Meißner, Int. J. Mod. Phys. E **4**, 193 (1995).
40. P. Büttiker and U.-G. Meißner, Nucl. Phys. A **668**, 97 (2000).
41. E. Epelbaum, U.-G. Meißner, and W. Glöckle, Nucl. Phys. A **714**, 535 (2003).
42. E. Epelbaum, U.-G. Meißner, and W. Glöckle, arXiv:nucl-th/0208040.

43. S. R. Beane and M. J. Savage, Nucl. Phys. A **717**, 91 (2003).
44. S. R. Beane, P. F. Bedaque, K. Orginos, and M. J. Savage, Phys. Rev. Lett. **97**, 012001 (2006).
45. S. R. Beane, P. F. Bedaque, M. J. Savage, and U. van Kolck, Nucl. Phys. A **700**, 377 (2002).
46. J.-W. Chen, T.-K. Lee, C.-P. Liu, and Y.-S. Liu, Phys. Rev. C **86**, 054001 (2012).
47. J. Soto and J. Tarrus, Phys. Rev. C **85**, 044001 (2012).
48. E. Epelbaum, U.-G. Meißner, W. Glöckle, and C. Elster, Phys. Rev. C **65**, 044001 (2002).
49. E. Epelbaum and J. Gegelia, arXiv:1301.6134 [nucl-th].
50. M. Frink, U.-G. Meißner, and I. Scheller, Eur. Phys. J. A **24**, 395 (2005).
51. J. M. Alarcón, J. Martin Camalich, and J. A. Oller, Phys. Rev. D **85**, 051503 (2012).
52. P. F. Bedaque, T. Luu, and L. Platter, Phys. Rev. C **83**, 045803 (2011).